

---

*Phase II Report*

**Geomorphic and  
Two-Dimensional Hydraulic  
Modeling Evaluation of the  
Little Miami River in the Eastern  
Corridor Segment II/III Study Area**

Submitted to

**Entran**

December 2009

Copyright 2009 by CH2M HILL, Inc.

**CH2MHILL** and



NewFields River Basin Services, LLC

---

# Table of Contents

Introduction and Purpose .....	1
1 Updated Hydrologic Analyses .....	1
2 Phase 2 Geomorphic Analyses .....	6
2.1 Meander Migration Rate Validation .....	6
2.2 Additional Meander Migration Rate Measurements .....	7
2.3 Meander Cutoff Analysis.....	11
3 Hydraulic and Sediment Transport Model Calibration and Phase 2 Analyses .....	13
3.1 Model Calibration Background .....	13
3.2 Low Flow Calibration .....	13
3.3 Medium Flow Calibration .....	18
3.4 High Flow Model Simulations.....	25
3.5 Sediment Transport Simulations.....	33
3.5.1 Inflow Sediment Concentration .....	34
3.5.2 Model Results .....	34
3.6 Geomorphic Interpretation of Hydraulic and Sediment Transport Modeling.....	37
4 Summary and Recommendations.....	38
References .....	39
Appendix A – Hydraulic Model Plan View Results .....	40

# Introduction and Purpose

---

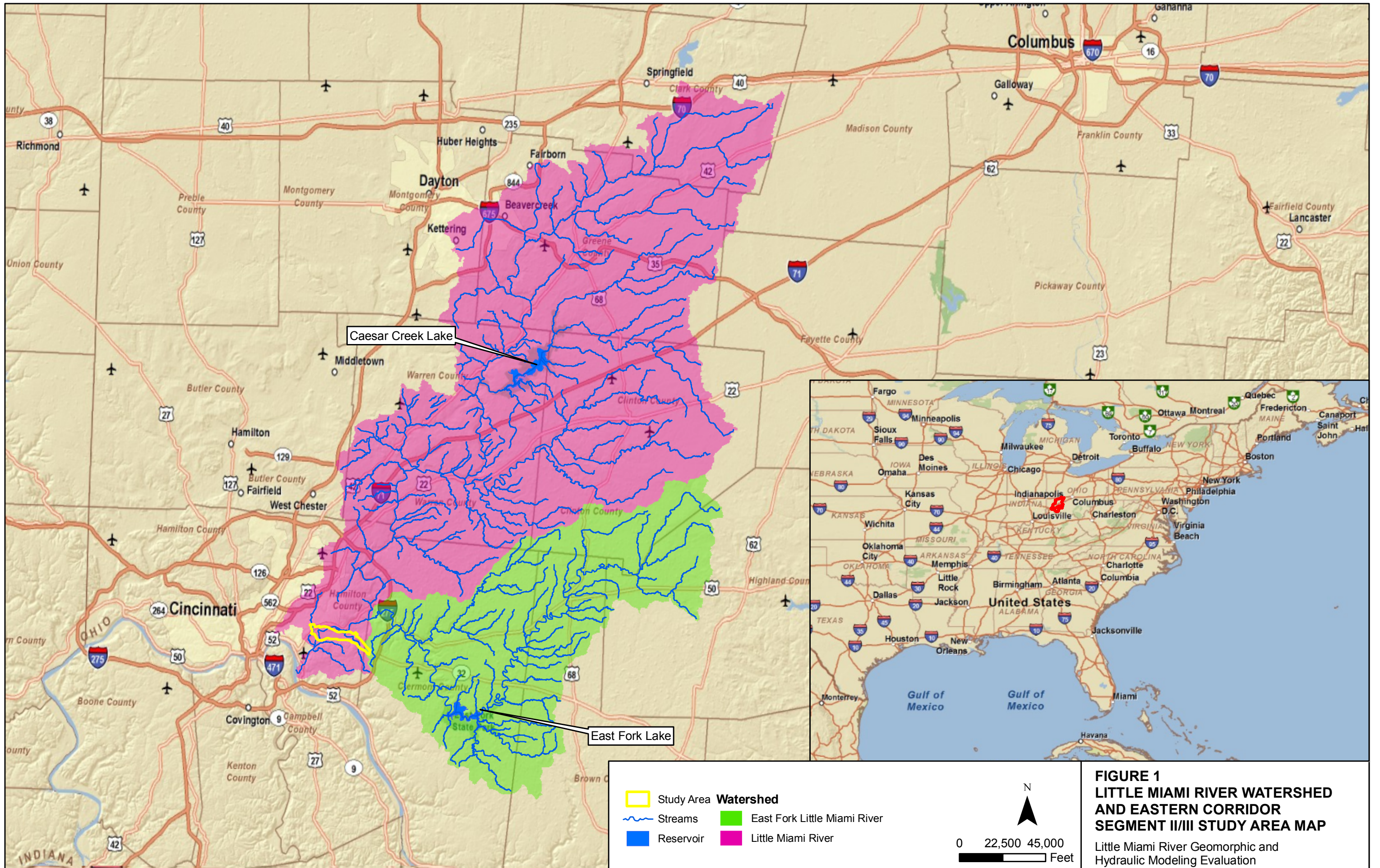
The first phase of this investigation (CH2M HILL 2009), conducted between September, 2008 and January, 2009, described the geomorphic setting, watershed hydrology, historical channel evolution, and hydraulic characteristics of the Wild and Scenic designated Little Miami River (Figure 1). Phase 1 included detailed analyses of watershed and site specific hydrology, geomorphology, hydraulics, and sediment transport, each conducted to evaluate the long-term stability of 2.5 miles of the Little Miami River (hereafter referred to as the Study Reach) in the general vicinity of “Horseshoe Bend,” an extreme meander in the river’s course where four potential bridge crossing locations have been proposed as part of the Segment II/III of the Eastern Corridor Investments (Figure 2).

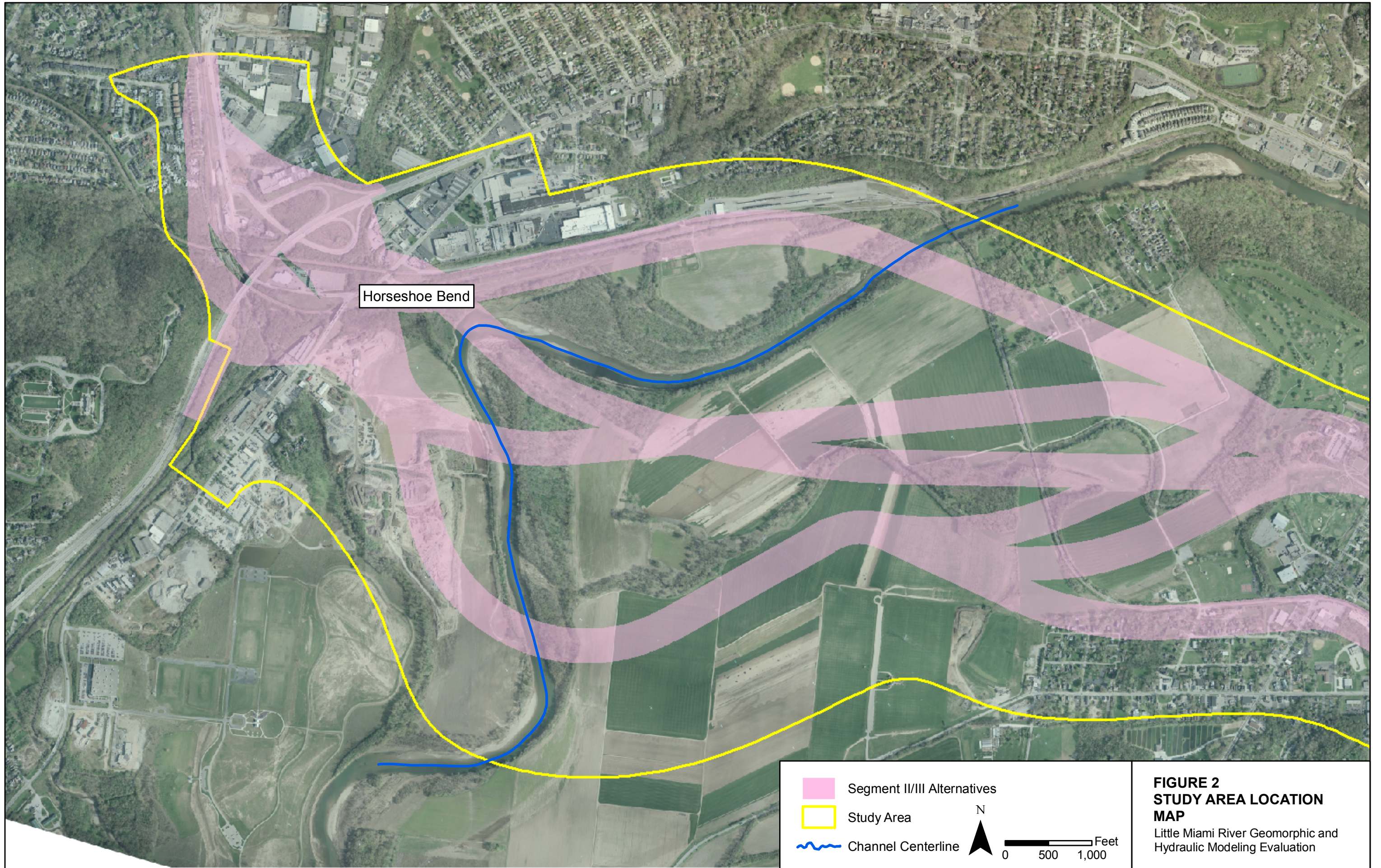
Phase 1 resulted in the prioritization of four geomorphic reaches with respect to their long-term stability, and therefore their suitability, for a clear span bridge crossing. Suitability ratings ranged from high (Geomorphic Reach 4) to moderate (Geomorphic Reach 7) to low (Geomorphic Reaches 5 and 6). The primary purpose of Phase 2 of this investigation was to validate and refine the analyses conducted in Phase 1 with additional data collection and analyses conducted between January, 2009 and November, 2009. Specifically, this included: 1) extension of hydrologic analyses with new flow data from the winter of 2008/2009; 2) refined historical channel morphology analyses in high and moderate suitability reaches, and validation of channel morphology analyses with empirical scour and erosion observations and calibrated hydraulic and sediment transport model results; 3) expanded analysis of potential channel meander cut-off dynamics and implications for high and moderate suitability reaches; and 4) calibration of hydraulic and sediment transport model with high flow water surface elevation data collected during the winter of 2008/2009.

## 1 Updated Hydrologic Analyses

---

The Phase 1 report (CH2M HILL 2009) details the hydrologic analyses conducted to develop an understanding of daily average flow, flood frequency, and flow concurrence characteristics in the Study Reach and its contributing watershed. In Phase 2, these analyses were amended with new streamflow data acquired from the United States Geologic Survey for the period between September 2008 and October 2009, for which streamflow data was not available at the time of the Phase 1 analyses. Data from USGS gage 03245500 “*Little Miami River at Milford OH*” and USGS gage 03247500 “*East Fork Little Miami River at Perintown OH*” were combined to produce hourly and peak flow records for the Study Reach. Figure 3 is a plot of daily mean discharge for the entire period of record, and Figure 4 is a plot of daily mean discharge for the study period and the four preceding years.





Horseshoe Bend

Segment II/III Alternatives  
 Study Area  
 Channel Centerline

N

Feet  
 0 500 1,000

**FIGURE 2**  
**STUDY AREA LOCATION**  
**MAP**  
 Little Miami River Geomorphic and  
 Hydraulic Modeling Evaluation

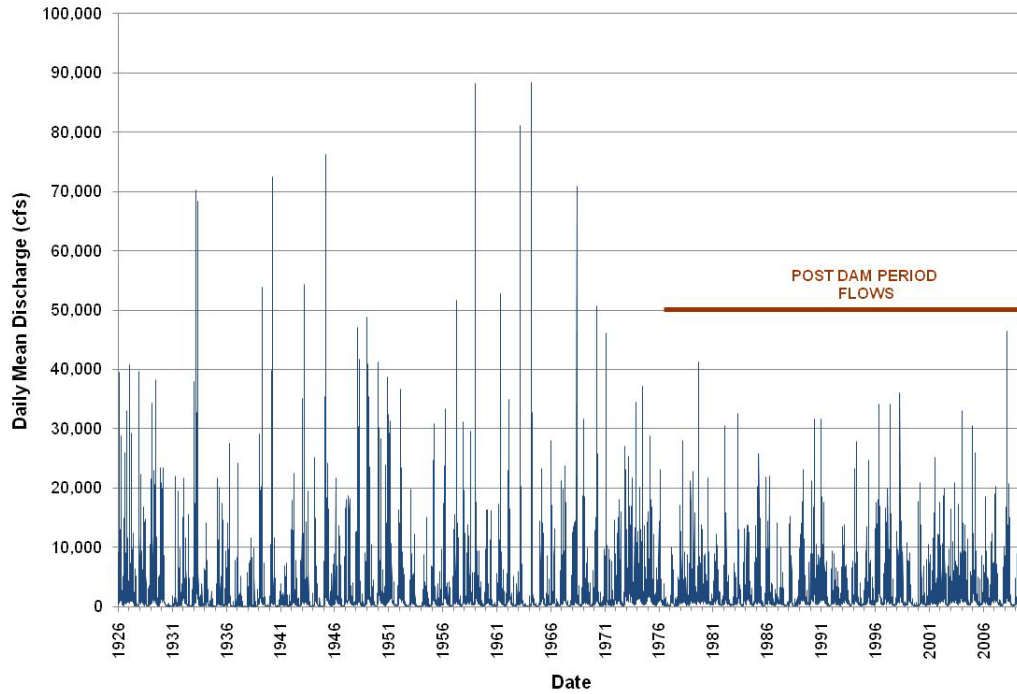


Figure 3: Daily mean discharge in the Study Reach (combined data from USGS gage 03245500 “Little Miami River at Milford OH” and USGS gage 03247500 “East Fork Little Miami River at Perintown OH”) for the period of record (1927-October 7, 2009).

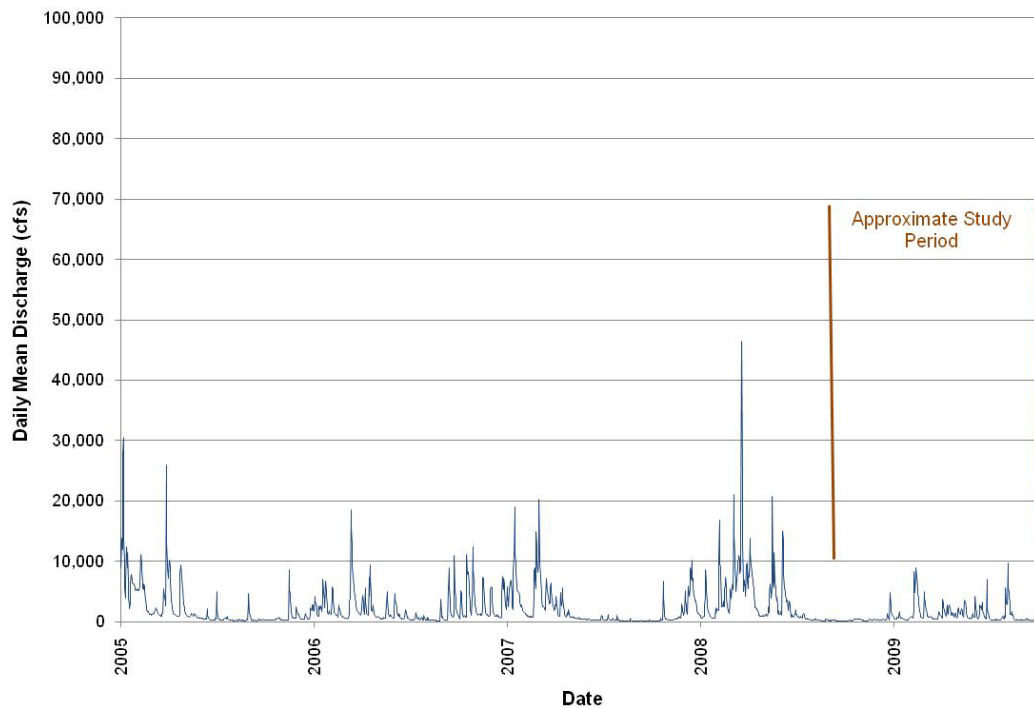
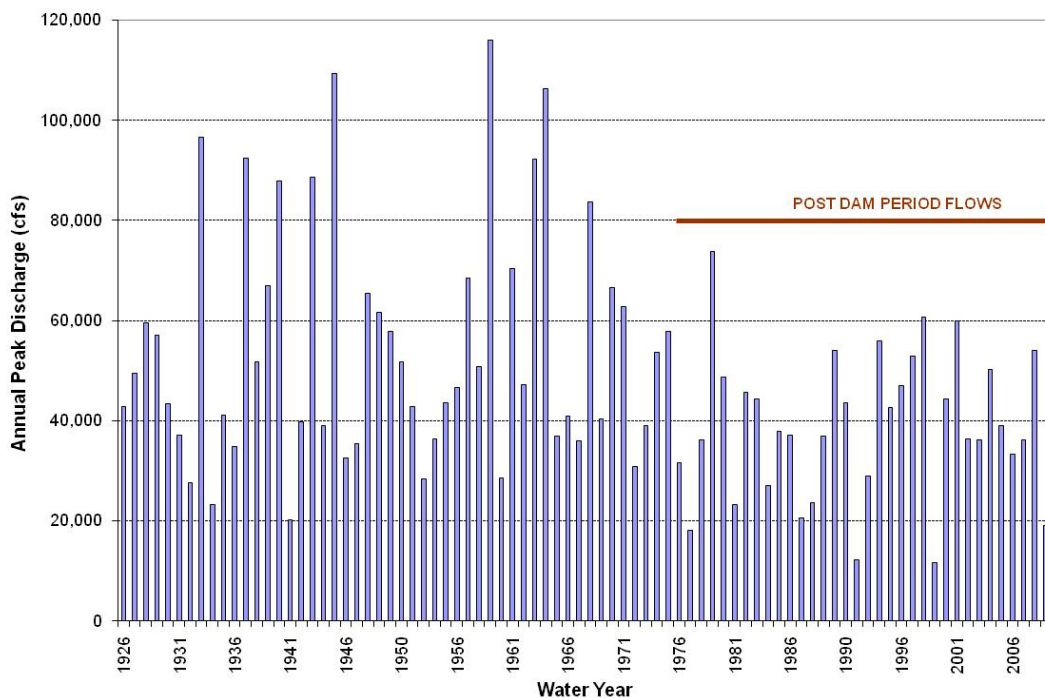


Figure 4: Daily mean discharge in the Study Reach (combined data from USGS gage 03245500 “Little Miami River at Milford OH” and USGS gage 03247500 “East Fork Little Miami River at Perintown OH”) for the five year period preceding and including the study period. Note that daily mean discharge is low during the study period relative to the preceding four years.

Figures 3 and 4 show that daily streamflow during the 2008/2009 study period was low relative to the preceding four years and the period of record. This provides hydrologic context for high flow scour and erosion measurements made by Stantec during the study period, which were used to help validate the long-term average meander migration rates calculated in Phase 1, and in the refinement of meander migration rates calculated in Phase 2 for the geomorphic reaches not eliminated in Phase 1.

The flood frequency analysis was also updated with peak discharges from 2008 and 2009 that were not available in Phase 1 of this analysis. Figure 5 shows the 2008 and 2009 peaks added to the record of peaks for the Study Reach. The 2008 peak occurred prior to initiation of this project but was not yet available from USGS at the time of the Phase 1 study. As illustrated in the daily mean discharge data, the annual peak flow during the study period was low relative to peaks of preceding years.



**Figure 5: Annual peak discharge in the Study Reach (combined data from USGS gage 03245500 “Little Miami River at Milford OH” and USGS gage 03247500 “East Fork Little Miami River at Perintown OH”) for the period of record 1927 to 2009. Note that peak discharge is low during the study period relative to the preceding nine years.**

Table 1 summarizes the amended flood frequency analysis. The addition of the 2008 and 2009 peak discharges did not significantly change the magnitude of discharges for recurrence intervals between one year and two hundred years. The additional peak discharges also match the patterns observed in the post-1975 flood frequency analysis results. Therefore, Phase 2 predictive analyses were conducted assuming that post-1975 hydrology is most representative of future conditions, as in Phase 1.

**TABLE 1**

Amended flood frequency analysis results for the Little Miami River for the period of record 1926 to October 7, 2009

Recurrence Interval (years)	Pre-1975 Discharge (cfs)	Full Record (1926-2009) Discharge (cfs)	Post-1975 Discharge (cfs)
1	19,684	13,355	9,529
2	49,913	45,176	38,524
5	71,194	64,664	52,089
10	86,078	76,716	58,790
25	105,689	90,974	65,257
50	120,851	100,908	68,963
100	136,530	110,260	71,928
200	152,773	119,227	74,365

## 2 Phase 2 Geomorphic Analyses

Three additional geomorphic analyses were conducted in Phase 2. First, field measurements of bank erosion made by Stantec (2009a) were used as a general validation of the long-term average channel meander migration rates calculated in Phase 1. Next, additional meander migration rates were calculated in the geomorphic reaches not eliminated in Phase 1 to provide improved guidance for final clear span bridge site selection. Finally, the potential for meander cut-off at the Horseshoe Bend identified in Phase 1 was evaluated in more detail to provide insights on potential impacts of alternative cut-off paths on adjacent geomorphic reaches.

### 2.1 Meander Migration Rate Validation

As described in Section 1 above, flow conditions were relatively low during the 2008/2009 study period, with daily mean discharge less than 10,000 cfs for the entire study period, and annual peak discharge of 19,080 cfs, which is less than a 1.5-year event. Therefore, assuming historical channel dynamics are reflective of current conditions, channel bank erosion distances measured by Stantec (2009a) during the study period should be similar to or less than average annual migration rates calculated in Phase 1 of this analysis. Channel bank erosion measurements from Stantec (2009a) were compared with historical channel migration rates from Phase 1 to assess the validity of the Phase 1 measurements. While field observations of bank erosion were too limited (both spatially and temporally) to eliminate uncertainty about potential future lateral channel migration, they can provide a check on the order of magnitude of lateral channel migration rates.

#### *Low Suitability Geomorphic Reaches*

Geomorphic Reaches five and six were determined to have low suitability for a clear span bridge crossing because of the relatively high lateral migration rate at the Horseshoe Bend (Geomorphic Reach 5) and the potential for upstream meander cutoff and subsequent large-scale channel change (Geomorphic Reach 6). Stantec (2009a) measured between zero and greater than 6 feet of erosion in Geomorphic Reach 5 (at the Horseshoe Bend) and only 0.22 feet of erosion at one location in Geomorphic Reach 6. Average annual lateral migration rates calculated in Phase 1 ranged from 1.5 feet to 16.8 feet (at the Horseshoe Bend) in Geomorphic Reach 5 and between 3.3 and 8.5 feet in Geomorphic Reach 6 (Table 3, CH2M HILL 2009). As expected for a relatively low study period peak flow of 19,080 cfs, the measured erosion distances were lower

than the historical Phase 1 average annual migration rates. While the measured erosion distances are lower than the average annual migration rates, they do show similar spatial distribution and order of magnitude of erosion, except in Geomorphic Reach 6 where measured erosion was an order of magnitude lower than the expected average annual lateral migration rate. Therefore, the field measurements of erosion can only be used to validate the long term average annual lateral migration rate for Geomorphic Reach 5. This supports the decision to eliminate Geomorphic Reach 5 from consideration. Because the measured erosion was lower than the already low average annual migration rate for Geomorphic Reach 6, the elimination of this reach from consideration should be justified by the potential for meander cutoff impacts, not by the expected local channel migration rate. Meander cutoff impacts are discussed in more detail in Section 2.3.

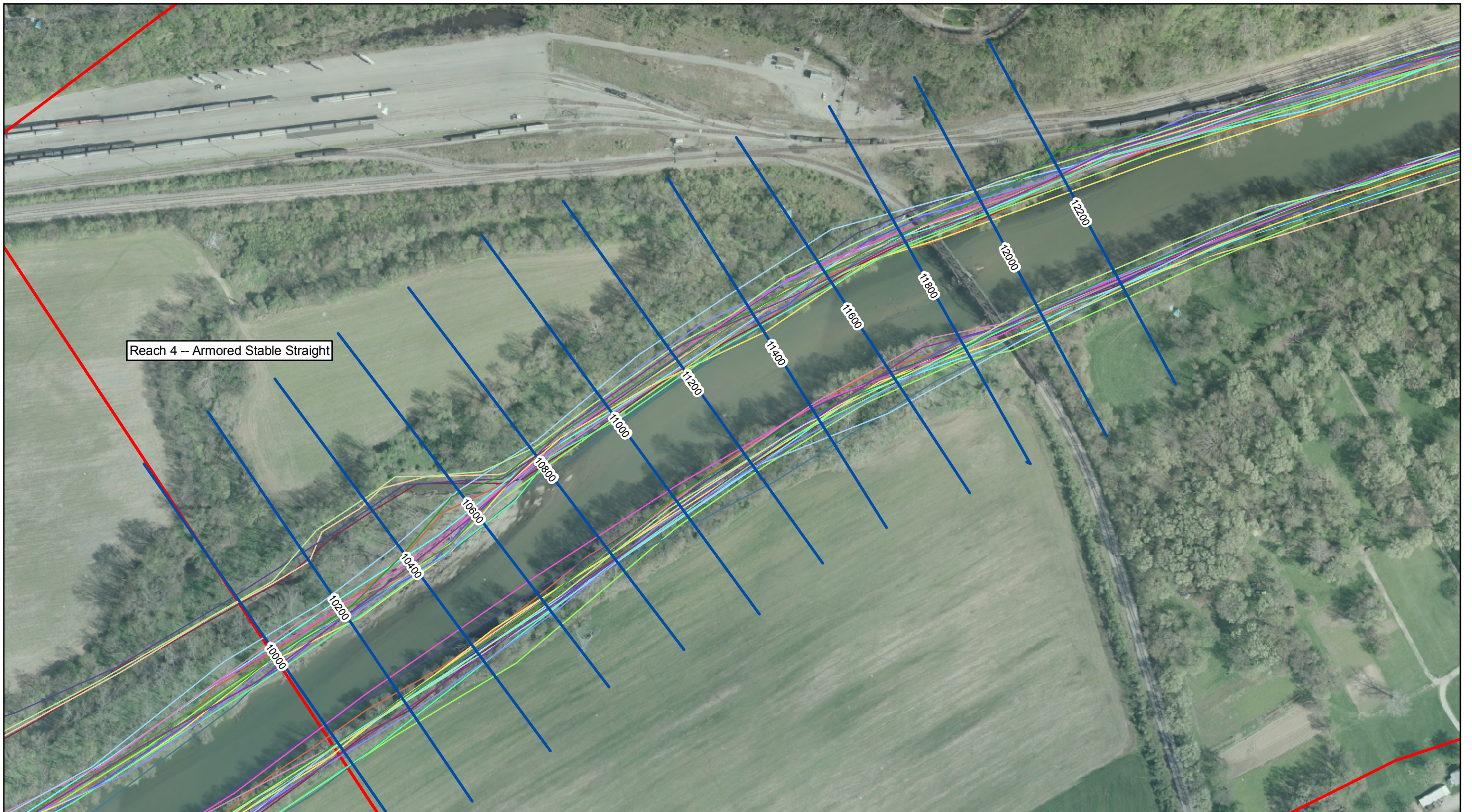
### ***High and Moderate Suitability Geomorphic Reaches***

Geomorphic Reaches 4 and 7 were determined to have high and moderate suitability, respectively, for a clear span bridge crossing because of the presence of sites with long-term stability in these reaches. Stantec (2009a) measured between 0.67 feet and 3.2 feet of bank erosion in Geomorphic Reach 7 and up to 0.25 feet of bank erosion in Geomorphic Reach 4. Average annual lateral migration rates calculated in Phase 1 ranged from 1.1 feet to 10.6 feet in Geomorphic Reach 7 and from 0.7 feet to 3.0 feet in Geomorphic Reach 4 (Table 3, CH2M HILL 2009). The measured erosion distances in both reaches were lower than the average annual migration rates calculated in Phase 1 but showed similar spatial distribution and order of magnitude of erosion. Therefore, the field measurements of erosion validate the long term average annual lateral migration rates calculated for these reaches in Phase 1. The relatively high measured erosion rate at the downstream end of Geomorphic Reach 7 and the corresponding average annual lateral migration rate confirm the finding in Phase 1 that only the upstream portion of Geomorphic Reach 7 should be considered suitable for a clear span bridge crossing. The low measured erosion rates and historical lateral channel migration rates in Reach 4 confirm the finding in Phase 1 that Reach 4 is the most suitable location for a clear span bridge crossing.

## **2.2 Additional Meander Migration Rate Measurements**

With a reasonable validation of lateral channel migration rates from Phase 1 completed, it was determined that additional measurements of historical meander migration could provide improved guidance for prioritization of clear span bridge crossing locations in Geomorphic Reaches 4 and 7. Figures 6 and 7 show transect locations and stations where additional meander migration rates were calculated using the techniques described in section 4.2 of the Phase 1 report (CH2M HILL 2009). Table 2 summarizes active channel widths and average annual lateral channel migration rates in locations still under consideration for a clear span bridge crossing. The active channel width is the width of the corridor bounded by the channel banks that are the farthest distance apart over the entire period of observation (1932 – 2007); the average annual lateral channel migration rate is the total distance of channel bank movement between 1932 and 2007 divided by the 75 year period of movement. Figure 8 illustrates how these values were measured.

This more refined analysis of historical channel migration provides improved information for prioritization of potential clear span bridge crossing locations in Geomorphic Reaches 4 and 7. While the Phase 1 meander migration rates did capture natural and anthropogenic channel change, the additional measurements in Phase 2 provides more site-specific estimates of historical lateral channel migration. In addition, this analysis provides a useful guide for establishment of minimum width requirements for the clear span portion of a new bridge. The active channel width should be considered the absolute minimum requirement for the clear span portion of the proposed bridge at a given location, and the average annual migration rate should be used as an index of the uncertainty in the prediction of the required clear span width over the design life of the bridge in



Reach 4 -- Armored Stable Straight

<b>Channel Extent</b>	1950	1968	1986	2004	Channel Migration Cross Sections
	1932	1975	1990	2005	Geomorphic Reaches
	1938	1962	1977	1994	2007
	1948	1964	1981	2000	

N

0 110 220 Feet

**FIGURE 6**  
**CHANNEL MIGRATION**  
**CROSS SECTIONS**  
 Little Miami River Geomorphic and Hydraulic Modeling Evaluation, Phase II



that location. For example, a bridge crossing at station 10,800 in Reach 4 would require a minimum 377 foot clear span section and a relatively low factor of safety to account for the low rates of average annual channel migration (1.1 ft/yr to 1.4 ft/yr) in this location. In contrast, a bridge crossing at station 1,600 in Reach 7 would require a minimum 922 foot clear span section and a relatively high factor of safety to account for the high rates of average annual channel migration (5.9 ft/yr to 8.6 ft/yr).

**TABLE 2**

Active channel widths and average annual lateral migration rate in geomorphic reaches 4, 6, and 7

Geomorphic Reach	Station (ft)	Active Channel Width 1932-2007 (ft)	Bank (looking downstream)	Average Annual Migration Rate (ft/yr)
7	0	1,408	Left	7.9
			Right	12.2
	200	981	Left	2.9
			Right	6.1
	400	703	Left	1.2
			Right	4.0
	600	778	Left	2.1
			Right	5.3
	800	829	Left	3.3
			Right	6.7
	1,000	857	Left	5.2
			Right	7.5
	1,200	879	Left	7.3
			Right	7.8
1,400	898	Left	8.4	
		Right	6.9	
1,600	922	Left	8.6	
		Right	5.9	
6	1,800	925	Left	8.5
			Right	4.9
	2,000	931	Left	8.8
			Right	4.3
	2,200	851	Left	7.4
			Right	3.6
	2,400	714	Left	5.6
			Right	3.2
4	10,000	489	Left	1.5
			Right	2.7
	10,200	497	Left	1.7
			Right	2.8
	10,400	524	Left	1.9
			Right	3.0
	10,600	450	Left	0.4
			Right	2.0
	10,800	377	Left	1.4
			Right	1.1
	11,000	393	Left	1.3
			Right	1.3
	11,200	428	Left	1.4
			Right	1.4
	11,400	434	Left	1.4
			Right	1.6
	11,600	446	Left	1.4
			Right	1.5
11,800	415	Left	1.2	
		Right	1.3	
12,000	388	Left	1.0	
		Right	1.1	
12,200	383	Left	1.0	
		Right	1.3	

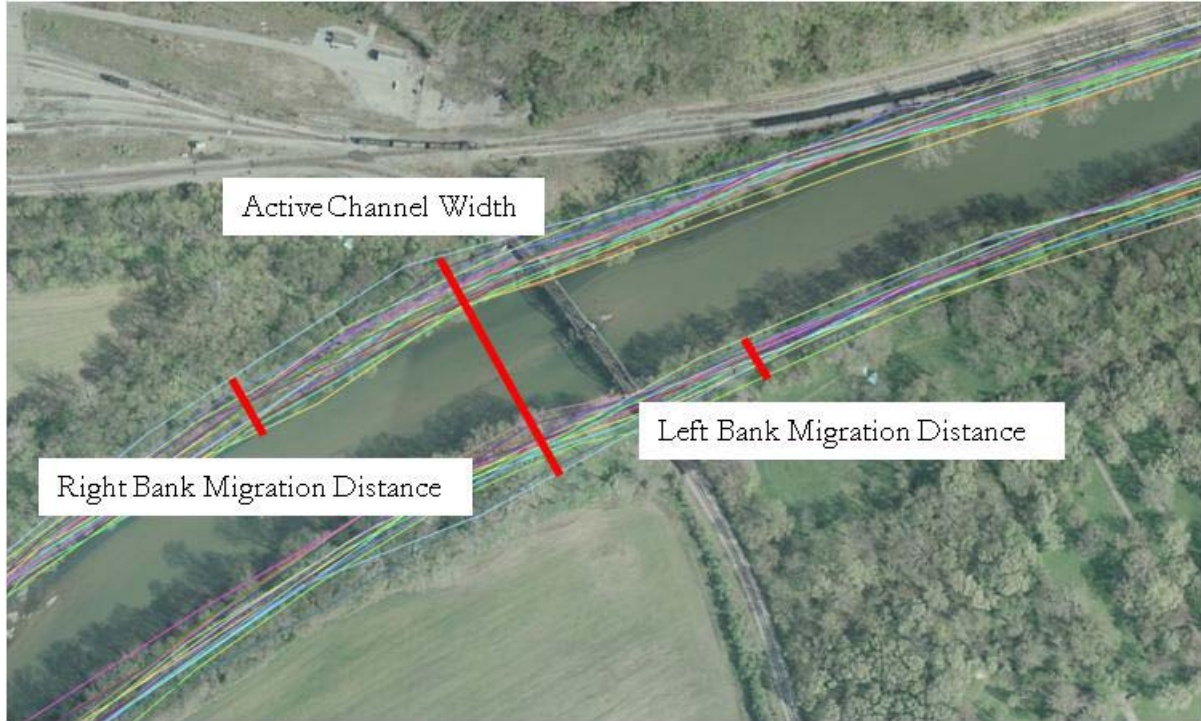
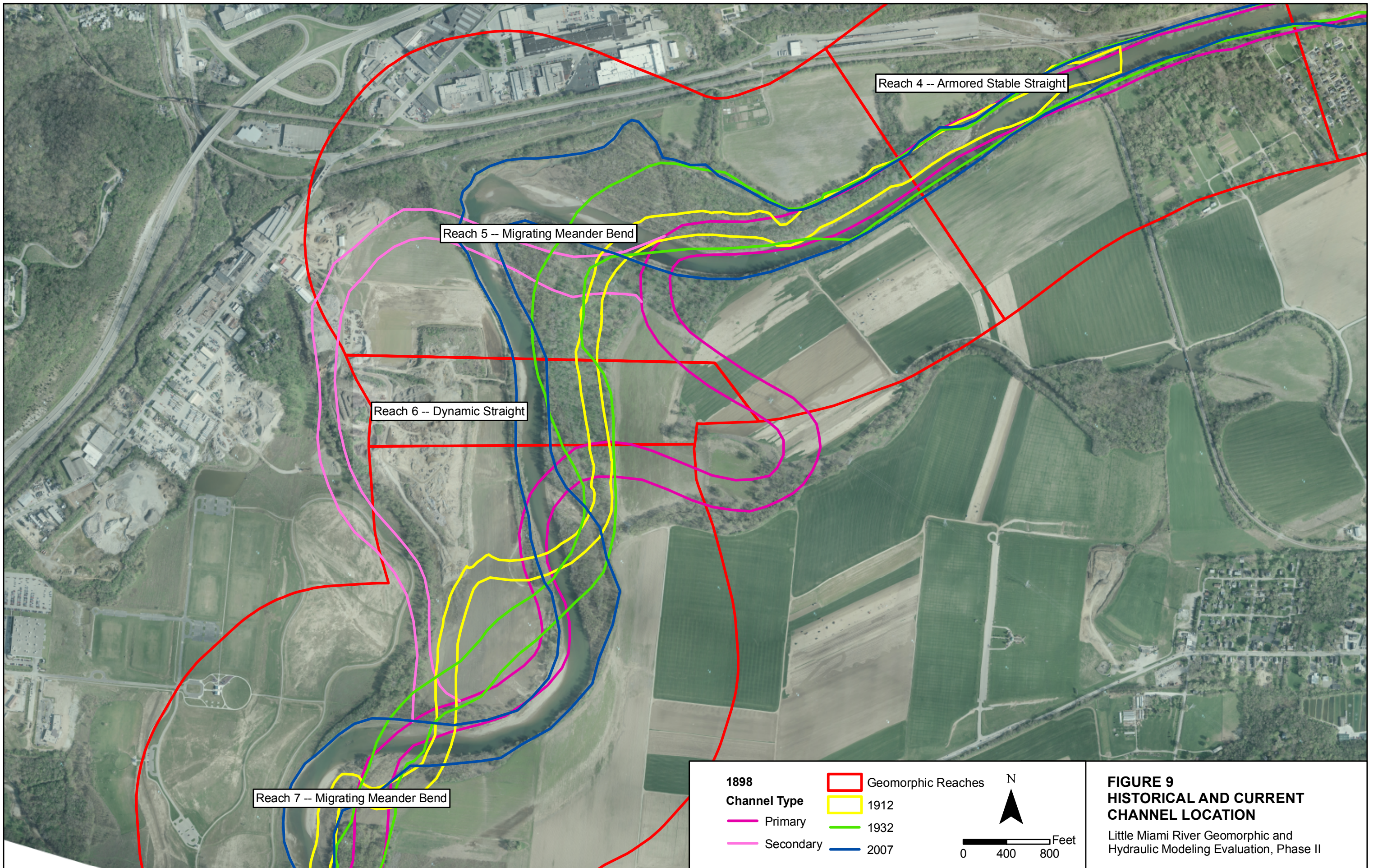


Figure 8: Schematic representation of active channel width and bank migration distances.

### 2.3 Meander Cutoff Analysis

Geomorphic analyses of historical maps, USGS topographic maps, and aerial photographs show that the Little Miami River has experienced significant channel migration, especially through the reach that includes Horseshoe Bend. This extreme meander bend has transitioned from an outside bend on the right side of the channel to an outside bend on the left side of the channel. As this bend continues to tighten and outward migration is arrested by riprap and other existing bank stabilization measures, a meander cutoff is likely in this location. To determine potential paths of a meander cutoff at the Horseshoe Bend, historical maps and aerial photographs were evaluated in GIS along with the calibrated hydraulic modeling results (discussed in Section 3). Figure 9 shows historical channel locations at Horseshoe Bend from 1898 to 2007.

Upstream of Horseshoe Bend in Geomorphic Reach 4, the channel has remained relatively stable over very long periods of time. Downstream of Horseshoe Bend in Geomorphic Reach 6, the channel has been influenced by the confluence with Clear Creek and secondary drainages along the Little Miami River floodplain. The 1898, 1912, and 1932 channel alignments in Figure 9 provide an estimate of potential future meander cut-off alignments. While there is almost certainly error in the alignments represented on the old maps, the historical channel alignments do provide reasonable boundaries for potential meander cutoff paths. Any meander cutoff would alter the local longitudinal slope of the channel and potentially induce significant channel change as hydraulics and sediment transport adjusted to the altered conditions. A cutoff could make the channel steeper or flatter locally, and would likely induce channel changes in upstream and downstream reaches similar to those observed in the past. Based on historical meander cutoff dynamics, Geomorphic Reaches 6 and 7 both appear extremely vulnerable to significant change with a new cutoff and are therefore not suitable for a clear span bridge crossing. Historical meander cutoff dynamics have not significantly influenced Geomorphic Reach 4. Therefore the suitability of this reach for a clear span bridge would remain high even with the assumption that a meander cutoff will occur over the life of the bridge.



**FIGURE 9**  
**HISTORICAL AND CURRENT**  
**CHANNEL LOCATION**  
 Little Miami River Geomorphic and Hydraulic Modeling Evaluation, Phase II

## 3 Hydraulic and Sediment Transport Model Calibration and Phase 2 Analyses

---

### 3.1 Model Calibration Background

The Phase 2 modeling analysis began with calibration of the hydrodynamic model. The objective of the calibration effort was to verify the adequacy of the geometric representation of the system by the model and the appropriateness of the model parameters specifying bed friction and eddy viscosity. The calibrated model increased confidence in model results and facilitated more detailed interpretation of model results than was possible in Phase 1. Two sets of water surface elevations surveyed by Stantec in 2009 were available to calibrate the model, one representing a low base flow and the other a moderate flow event. Flow data used in the calibration effort was comprised of flow measurements from two USGS gages upstream of the project site. USGS gage 03245500 is located in Milford, Ohio, approximately 6.1 miles from the upstream end of the model domain at the railroad bridge. USGS gage 03247500 is located at Perintown, Ohio, on the East Fork, approximately 9.6 miles upstream from the railroad bridge.

### 3.2 Low Flow Calibration

Field surveys were conducted between 10/13/2008 and 10/17/2008 to measure channel transect and thalweg elevations in the project reach. The survey recorded water depths and water surface elevations at each survey point. These water surface elevations comprise the first calibration dataset. The field survey was initiated at the upstream end of the project reach and progressed downstream. Figure 10 shows the dates on which transects were surveyed. Figure 11 presents the average daily flow as measured at the Milford and Perintown USGS gages, as well as the combined flow for an eleven day period around the days of the low flow survey. Flow was nearly constant during the first three days of the survey (10/13 to 10/15), but increased on 10/17/08, apparently with a release from a reservoir on the East Fork (note the constant flow after 10/17).

Figure 12 shows the water level survey data interpolated onto the model grid. Note the steep gradient just upstream of Horseshoe Bend. At low flows, this section of the Study Reach forms a shallow riffle. This riffle exerts considerable friction on the flow, and thus the Manning's n-value (friction coefficient) was increased from the value used in Phase 1. The increased roughness in this reach more accurately depicts low flow channel morphology. A new material type was created to represent the riffle, and a sensitivity study was conducted to determine the influence on predicted surface water profiles of incremental changes in the Manning's n-value for this section of the channel. The location of the riffle material added for the low flow calibration simulations is shown in Figure 13.

The calibration simulation used an inflow of 186 cfs, the average river flow during the first three days of the water level and thalweg survey. Since the downstream water levels reflect the increased flow on October 17<sup>th</sup>, the downstream boundary was set 0.5 feet below the survey measurement. This adjustment was based on a review of the stage-discharge curve at the Milford gage. The calibration adjusted the Manning's n-value in the riffle section in order to match the water surface elevations measured on October 13, 14, and 15. Figure 14 presents the results of the final two calibration simulations, with Manning's n-values of 0.06 and 0.10 in the shallow riffle zone. Model results with an n-value of 0.06 minimize the root mean square error (RMSE) between predicted and measured water surface elevations. The RMSE for  $n = 0.06$  was calculated at 0.31 feet. Figure 14 shows that a Manning's n-value of 0.10 for the low flow riffle increases water surface elevations by up to 0.25 feet compared to the final calibration simulation with  $n = 0.06$ . Table 3 presents a summary of Manning's n-values for various channel substrates (FHWA 1986). For depths of less than 0.5 feet and a substrate of 2 inch gravel, the table suggests a Manning's n-value of 0.066. This is similar to the value used in the calibration simulation.

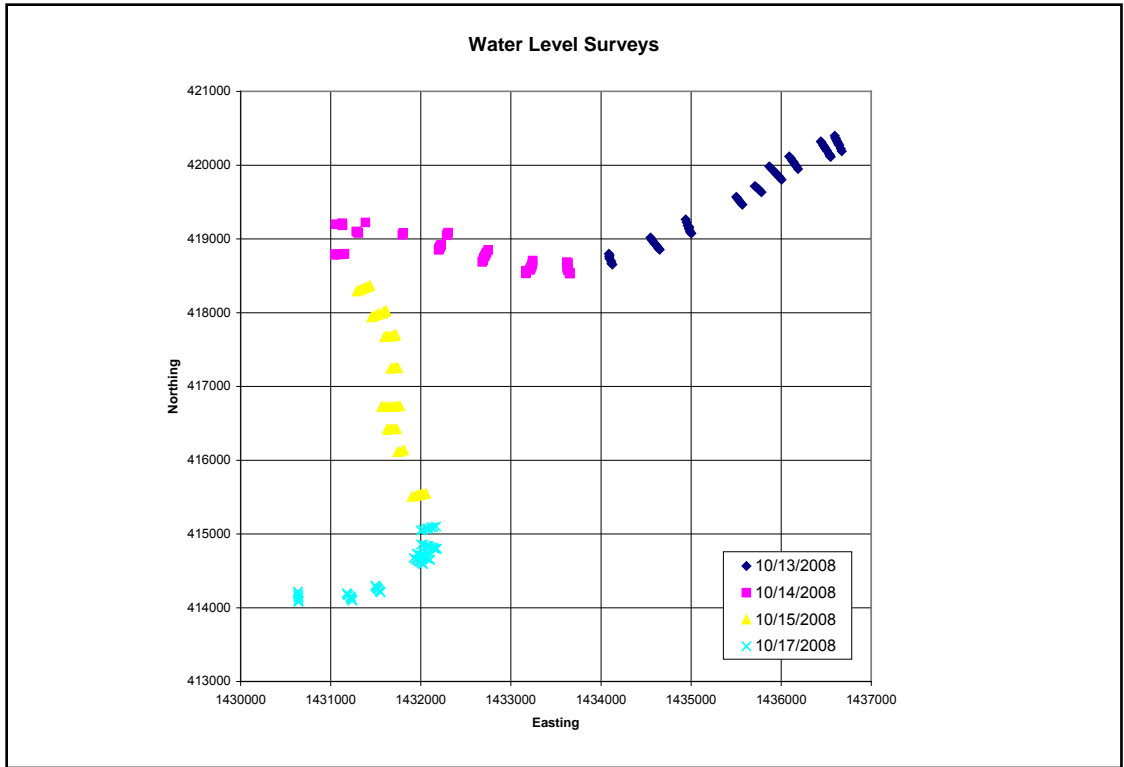


Figure 10: Low flow bathymetry and water surface elevation transect in Study Reach (October 2008)

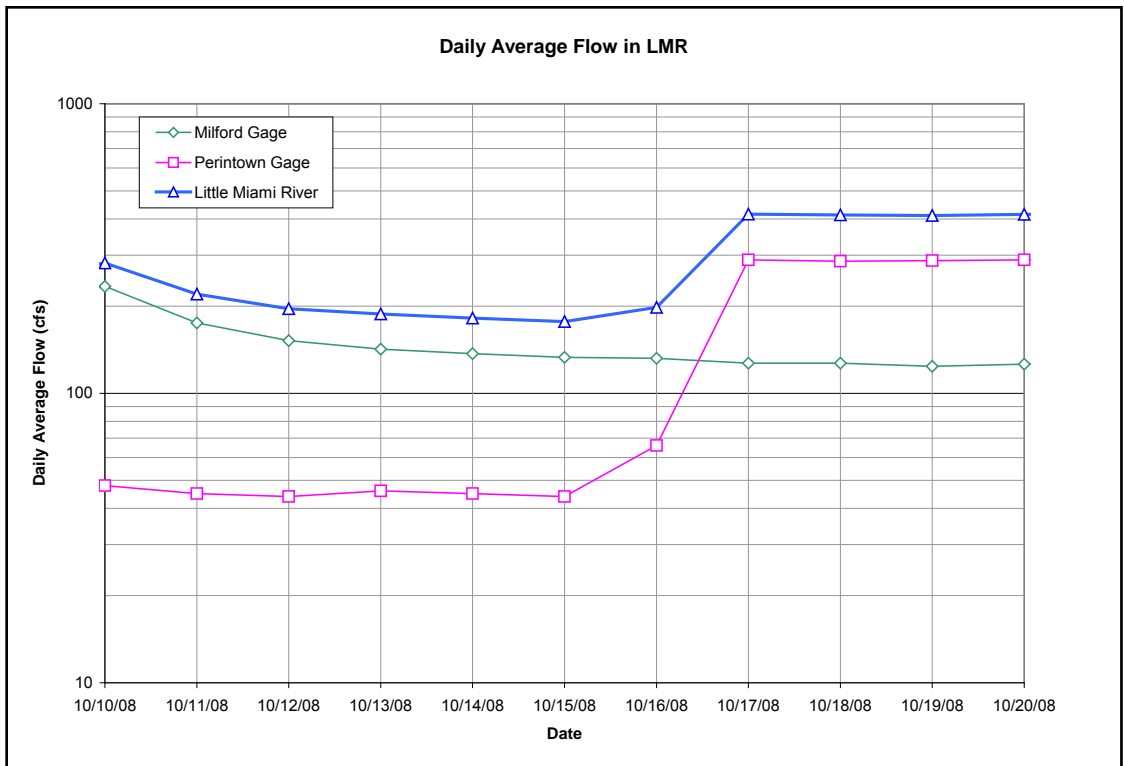


Figure 11: Flow in Little Miami River during low flow survey



Figure 12: Interpolation of water surface survey data onto model grid

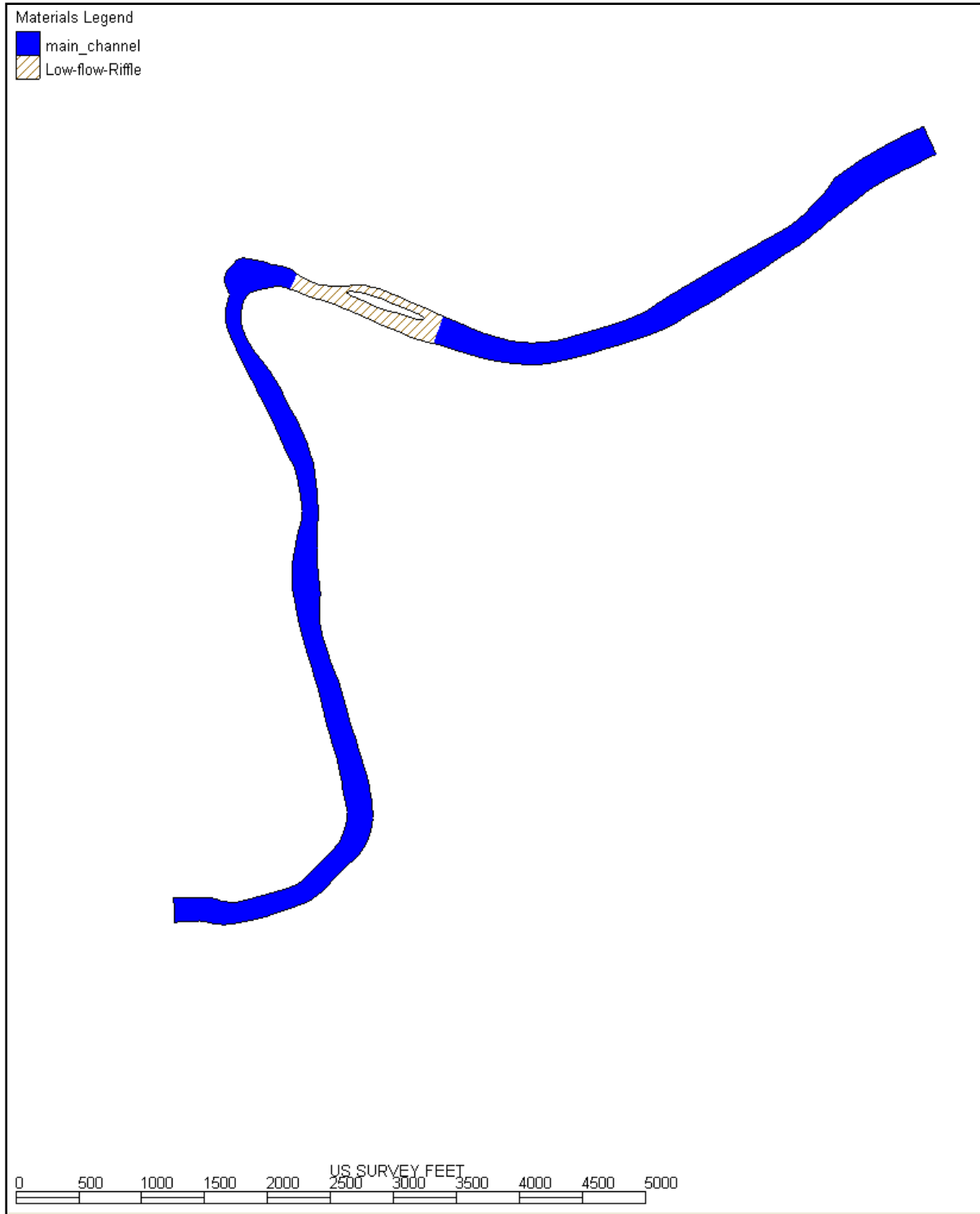


Figure 13: Material type distribution in low flow grid showing location of new riffle material

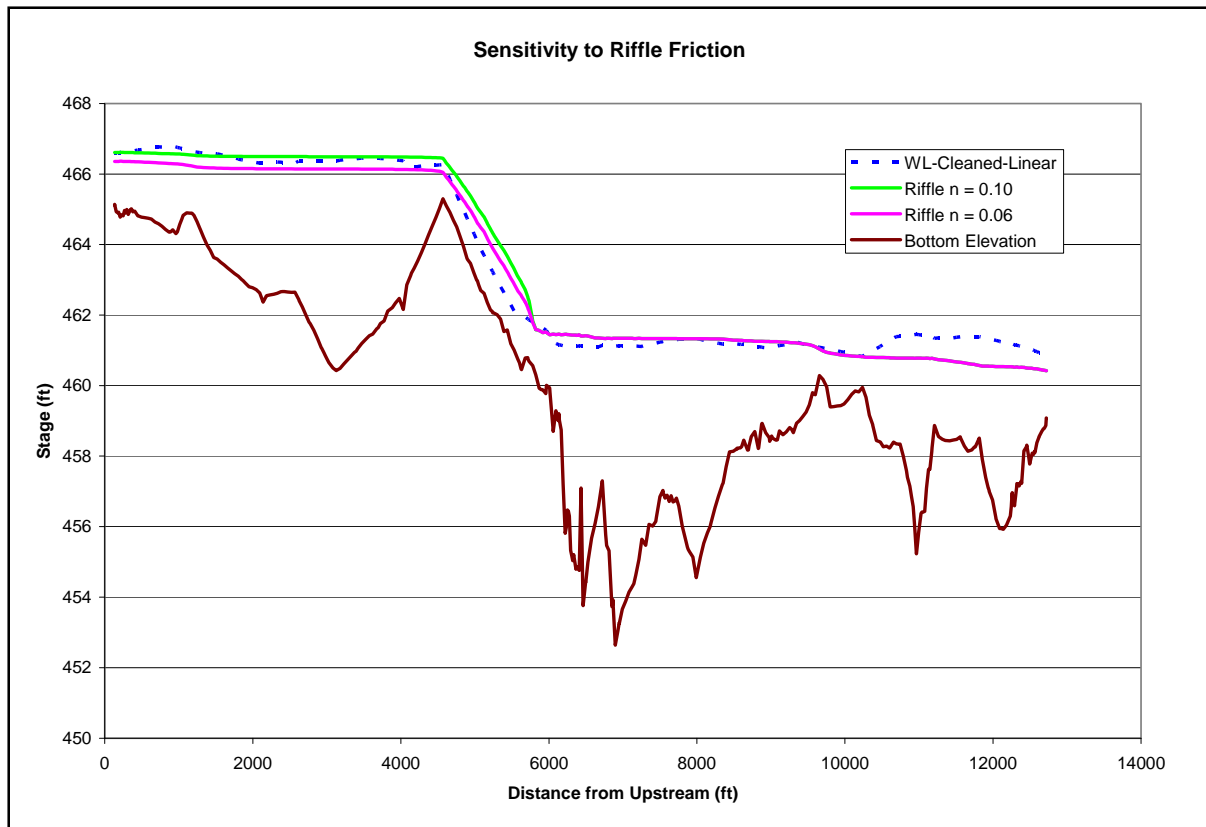


Figure 14: Final calibration and sensitivity to Manning's n-value in shallow riffle

**TABLE 3**

Manning's n-values for artificial channels used to guide roughness assignments for model calibration (FHWA 1986)

Category	Lining Type	Depth Ranges		
		0 – 0.5 ft	0.5 – 2.0 ft	> 2.0 ft
Rigid	Concrete	0.015	0.013	0.013
	Grouted Riprap	0.040	0.030	0.028
	Stone Masonry	0.042	0.032	0.030
	Soil Cement	0.025	0.022	0.020
	Asphalt	0.018	0.016	0.016
Unlined	Bare Soil	0.023	0.020	0.020
	Rock Cut	0.045	0.035	0.025
Temporary*	Woven Paper Net	0.016	0.015	0.015
	Jute Net	0.028	0.022	0.019
	Fiberglass Roving	0.028	0.022	0.019
	Straw with Net	0.065	0.033	0.025
	Curled Wood Mat	0.066	0.035	0.028
	Synthetic Mat	0.036	0.025	0.021
Gravel Riprap	1-inch D <sub>50</sub>	0.044	0.033	0.030
	2-inch D <sub>50</sub>	0.066	0.041	0.034
Rock Riprap	6-inch D <sub>50</sub>	0.104	0.069	0.035
	12-inch D <sub>50</sub>		0.078	0.040

Note: Values listed are representative values for the respective depth ranges. Manning's roughness coefficients, n, vary with the flow depth.  
\*Some "temporary" linings become permanent when buried.

### 3.3 Medium Flow Calibration

The second flow calibration was conducted with water surface elevations surveyed on June 26, 2009. Flow in the Little Miami River varied considerably on June 26, 2009, from a low of 721 cfs at 2:00 AM to a peak at 7:00 AM of 17,950 cfs. Flows declined quickly to 8,430 cfs at 12:00 noon, and then more gradually to 4,000 cfs by 6:00 PM. A field survey was conducted on June 26, 2009 to measure elevated water surface elevations caused by the high flow event. Measurements were taken at five points between 10:45 AM and 2:04 PM. The hourly flow, derived by combining measurements at the Milford and Perintown USGS gages, is shown in Figure 15.

The location and timing of the water level survey points are presented in Figure 16. The survey began on the north bank near the railroad bridge, with the first point being measured at 10:45 AM. Water levels at the Horseshoe Bend were recorded at 11:36 AM. Two locations on the south bank in the upper half of the model reach were surveyed at 1:00 PM and 1:14PM. The final survey point near the downstream end of the project reach was taken at 2:04 PM.

The river flow was decreasing rapidly during the water level survey. The hydrodynamic model input requires specification of flow at the upstream end of the model domain and water level at the downstream end. Since only one water level measurement was available at the downstream end for use in specifying the stage boundary, the calibration effort was conducted as a series of four model simulations. The first simulation used the measured downstream stage (467.11 ft) and an estimate of the river flow at the time the water level measurement was made. Successive model simulations were conducted with estimates of the downstream stage and river flow at the times the other high water surface elevations were surveyed.

The measured river flows were lagged before being applied as upstream boundary conditions in the numerical model. In order to determine an appropriate lag time between the combined flows measured at the upstream gages and the flow at the upstream end of the model (railroad bridge), records of measured flows at two gages on the north fork of the Little Miami River were analyzed. Data from the USGS website were downloaded for a 60 day period (8-14-2009 to 10-13-2009) at Milford (USGS gage 03245500) and Spring Valley (USGS gage 03242050). Measured stage at these two gages, recorded every 30 minutes, was compared graphically (Figure 17). The lag time between local peaks in the stage record were compared to determine the travel time between the two gages, located approximately 47.8 miles apart. An example of this analysis is presented in Figure 18.

The analysis was conducted for six distinct events. Results of the analysis are summarized in Table 4. The average lag time for the six events was 9.6 hours. Assuming that linear interpolation is appropriate, the average lag time was scaled to reflect the distance from the Milton gage to the upstream end of the model (48 miles vs. 6 miles), yielding an average lag time of 1 hour. The flow at Milton peaked ahead of the flow at Spring Valley in three of the six records, indicating a possible rainfall event contributing runoff between the Spring Valley and Milford gages. Review of historical data indicates that stage increased first at the Milton gage and then at the Spring Valley gage on June 26, 2009.

Model inflows used in the calibration simulations were linearly interpolated from hourly flows, assuming a one hour lag between the measured flows to account for travel time to the model boundary, as shown in Figure 19. Once the flows were determined, the stage-discharge curve derived for the Milford gage, presented in Figure 20, was used to estimate an appropriate increase in the downstream stage. The change in stage for a given increase in flow at the model boundary was assumed to equal the change in stage at Milford for the same increase in flow. For example, the stage-discharge equation at Milford predicts an increase in water level of 0.61 feet for an increase in flow from 7215 cfs to 8430 cfs. This same increase was applied at the downstream stage boundary for the same increase in flow. Table 5 summarizes the flow and stage boundary conditions used in the calibration simulations. Steady state runs were conducted as opposed to routing the flood hydrograph through the model because of the lack of information on the variation in downstream stage with flow. The assumption that the stage-discharge relationship at Milford is representative of the stage-discharge relationship at the model boundary (relative to a different datum) was necessary to proceed with the analysis.

Results of the four calibration simulations are presented in Figure 21 along with the surveyed water surface elevations. Considering the limited data and the assumptions required to determine boundary flows and stages, the calibration results appear reasonable. These results indicate that the model parameters for friction and eddy viscosity applied in Phase 1 of the modeling study were appropriate. Therefore, no adjustments to Manning's  $n$  were made in this calibration. The model grid was adjusted during the calibration effort for the June 26 flow event. An iterative approach was used to reduce the model grid based on predicted water depths such that the model correctly represented the proper flow width. A final review of the model's sensitivity to the eddy viscosity parameter was conducted. The final calibration simulation used a Peclet number of 20 to automatically specify the eddy viscosity on an element by element basis, a default recommended value (USACE 2009). Figure 22 indicates that for a reasonable range in Peclet numbers, the predicted water surface elevations varied by less than 0.5 feet.

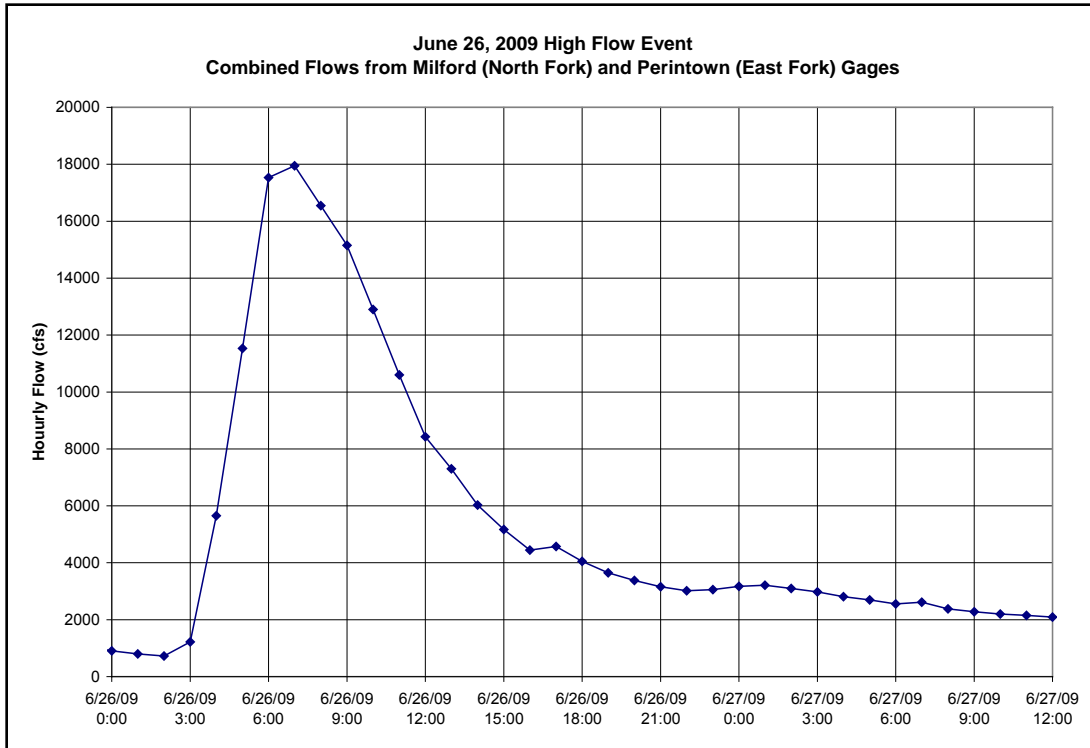


Figure 15: Little Miami River flow on June 26, 2009

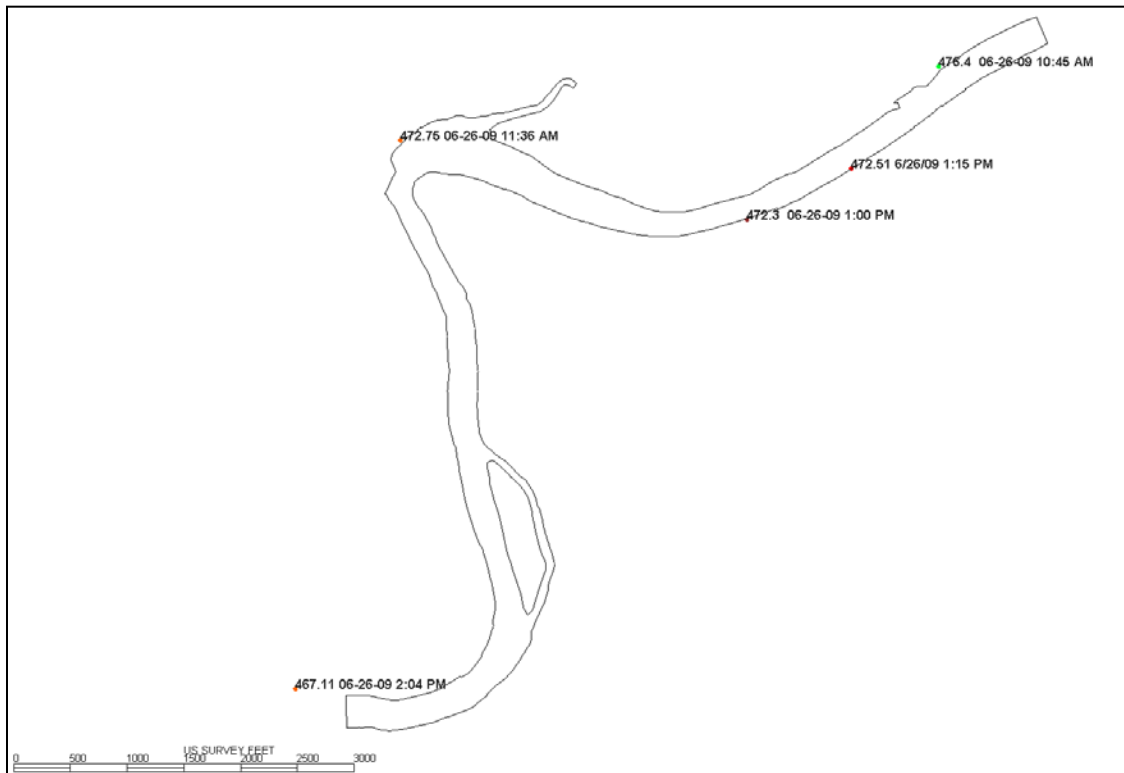


Figure 16: Location and elevation of water level survey points on June 26, 2009

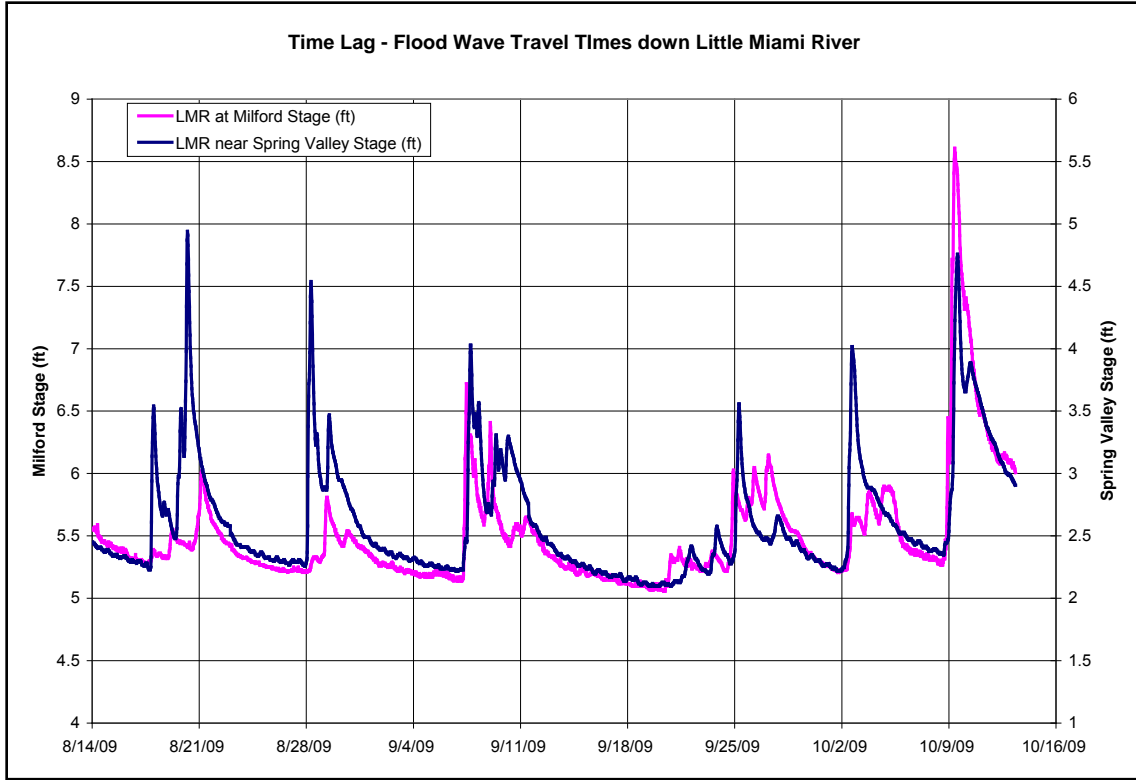


Figure 17: Stage records used to determine lag time for measured flows

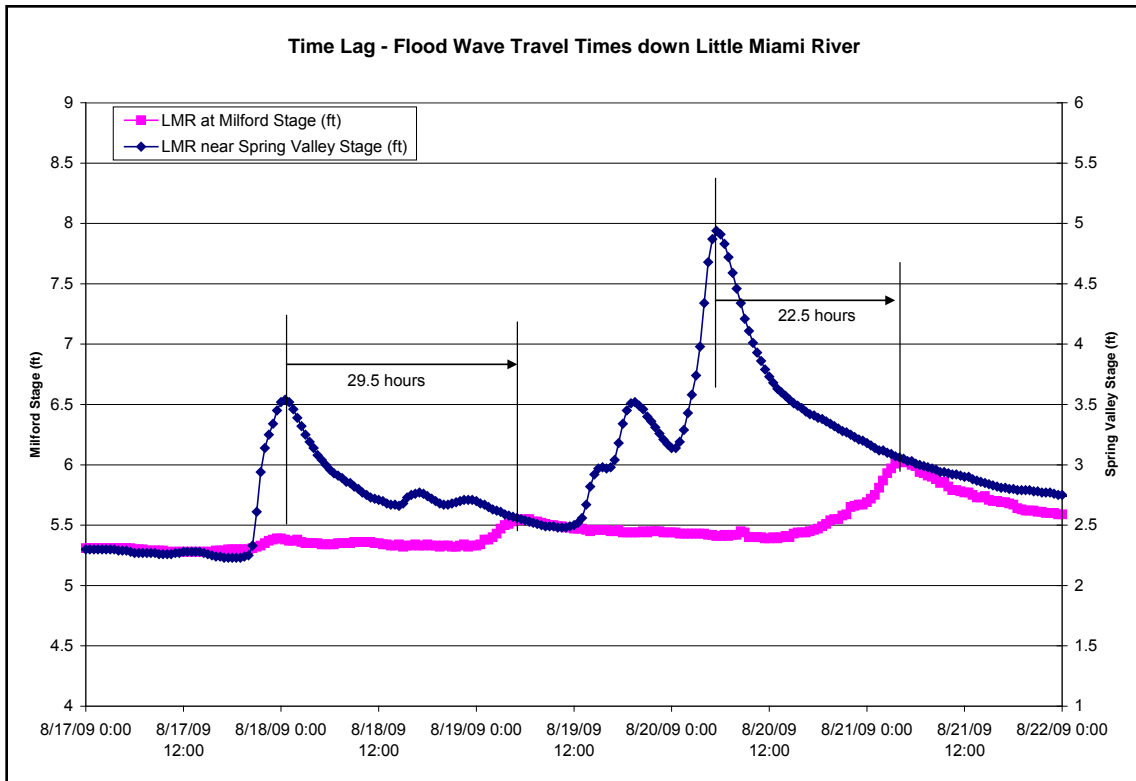


Figure 18: Example of lag time calculations

**TABLE 4**

Summary of time lag analysis

Spring Valley Gage	Milton Gage	Lag Time (hrs)	Milton Flow (cfs)	East Fork Flow (cfs)
8/18/2009 0:30	8/19/2009 6:00	29.50	331	56
8/20/2009 5:30	8/21/2009 4:00	22.50	618	56
8/28/2009 7:30	8/29/2009 8:30	25.00	476	41
9/7/2009 17:30	9/7/2009 11:00	-6.50	1270	63
9/25/2009 6:30	9/24/2009 22:00	-8.50	626	381
10/9/2009 13:30	10/9/2009 9:00	-4.50	4790	3710
Average		9.6		

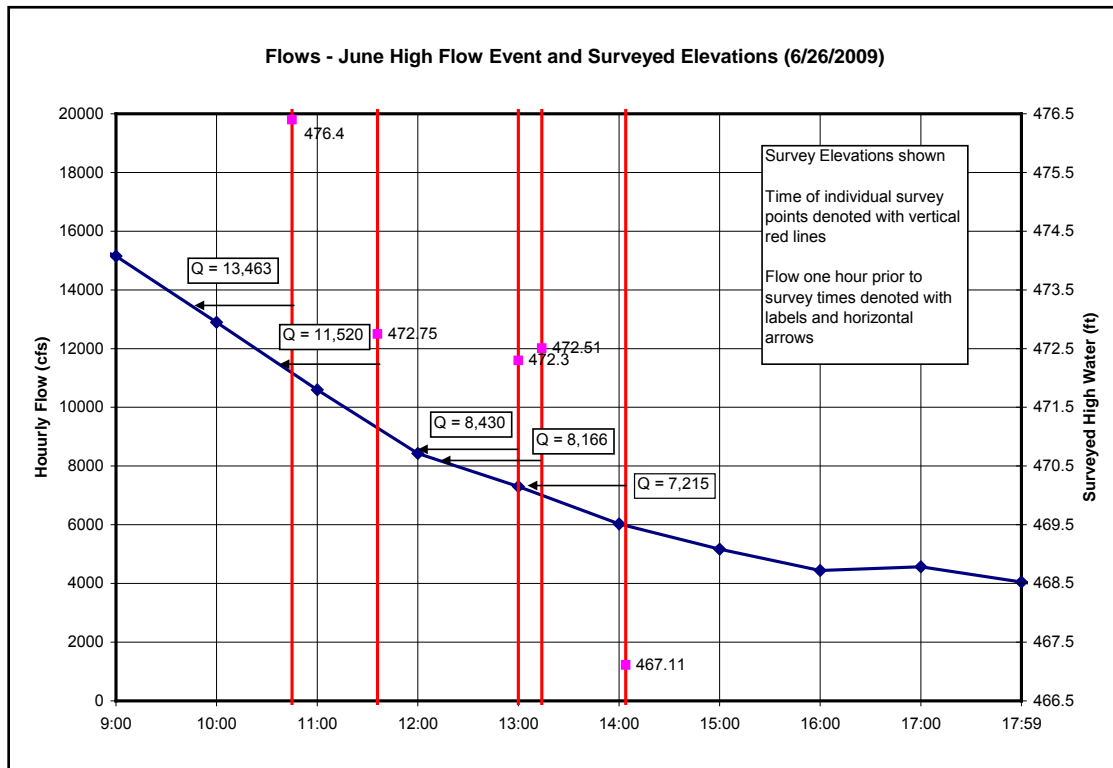


Figure 19: Calibration inflows and water surface elevation survey times

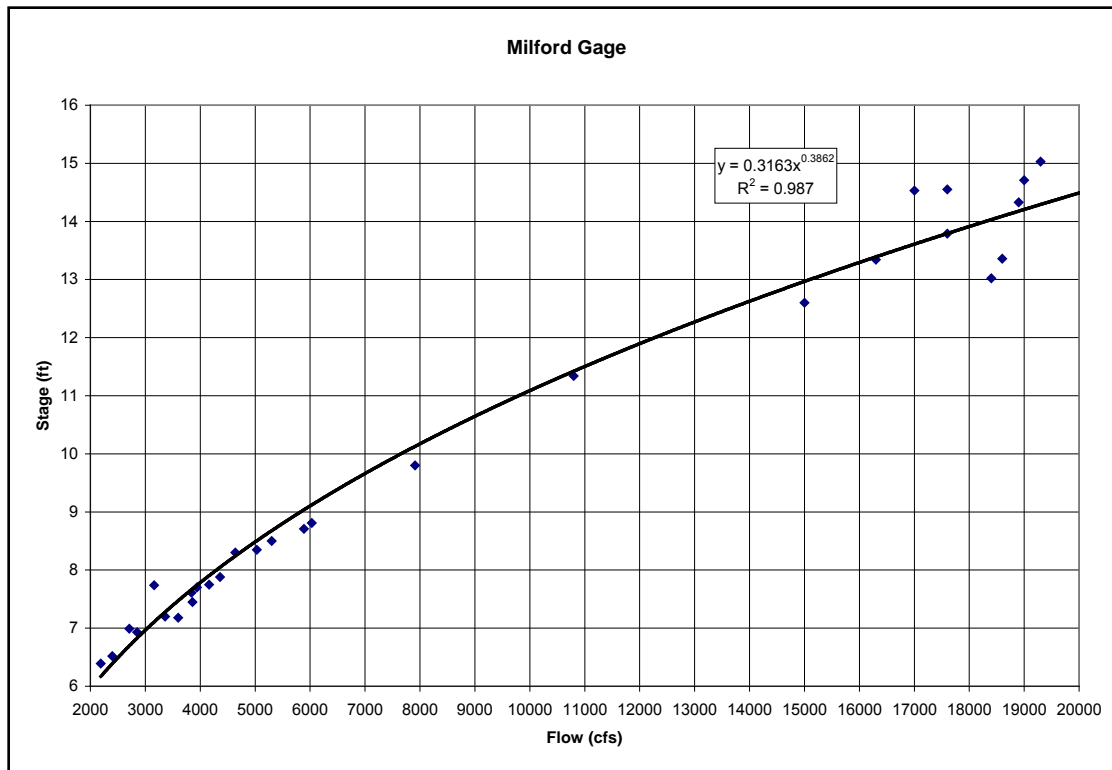


Figure 20: Stage discharge curve for Milford Gage, Little Miami River

TABLE 5

Summary of boundary conditions for June 26 calibration simulations

Model Run ID	Sample Time	Inflow (cfs)	Downstream Stage (ft)
Hi_04b	2:04 PM	7,215	467.11
Hi_04d	1:00 PM	8,430	467.72
Hi_04c	11:36 AM	11,520	469.05
Hi_04	10:45 AM	13,463	469.77

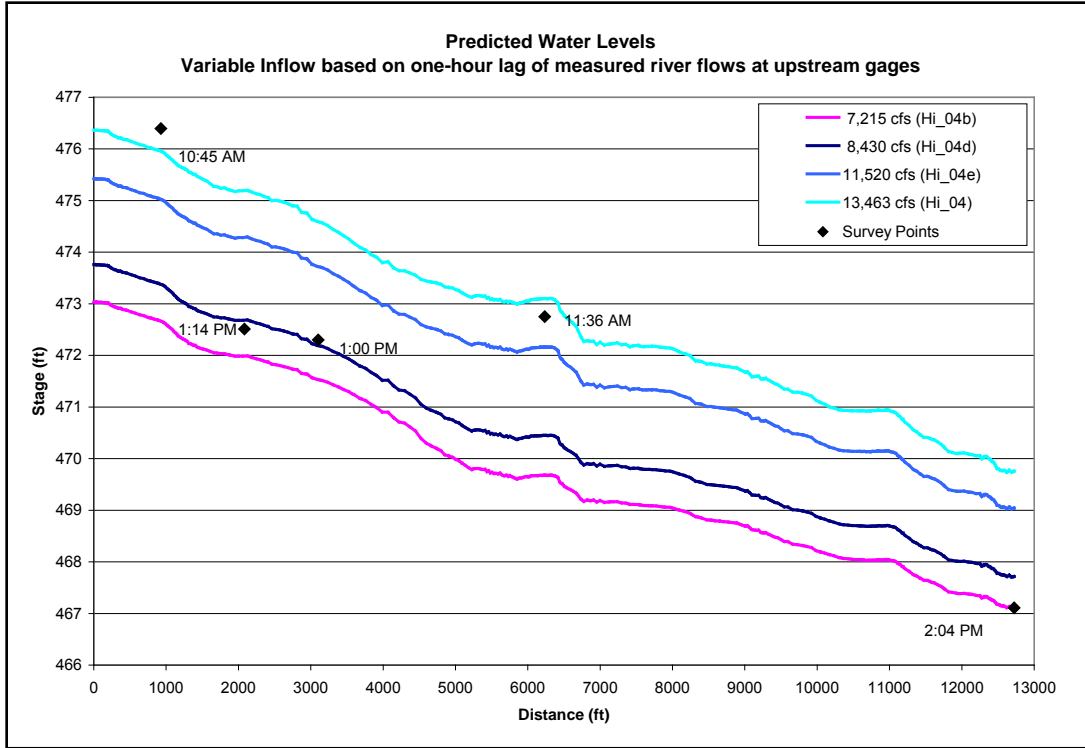


Figure 21: Calibration results - predicted water profiles and calibration survey points

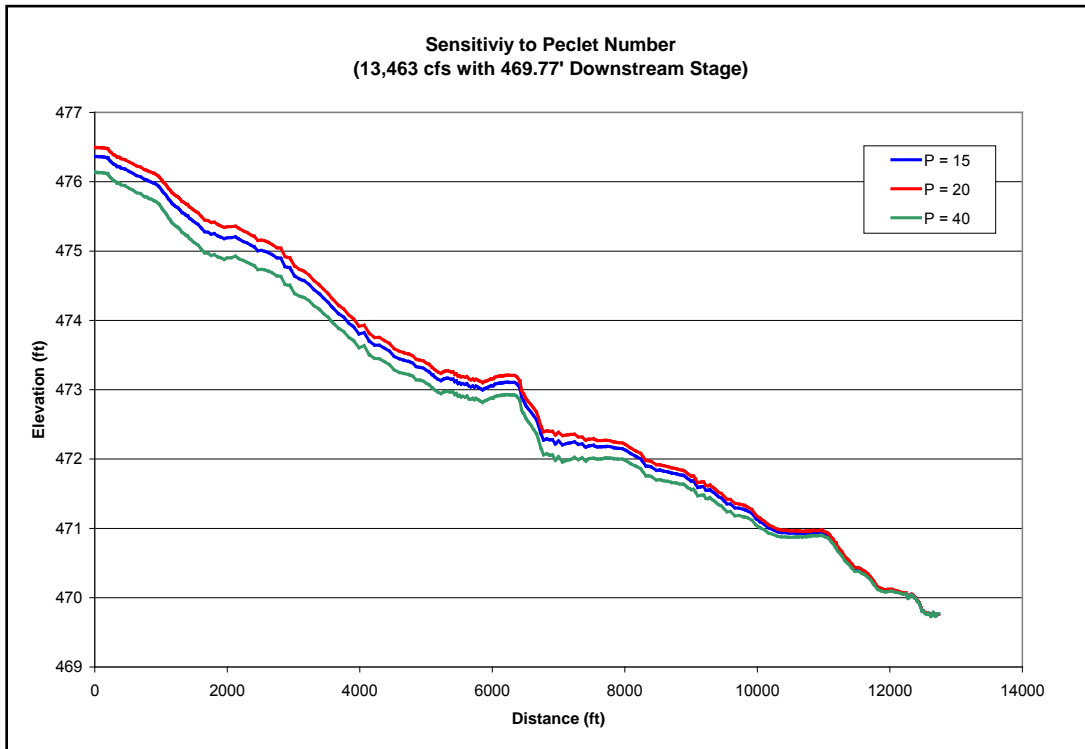


Figure 22: Sensitivity to Peclet Number (eddy viscosity)

### 3.4 High Flow Model Simulations

Three flows were selected for hydrodynamic and sediment transport modeling in Phase 2: 10,000 cfs, 45,000 cfs, and 65,000 cfs. The 10,000 cfs flow (approximate 1-year recurrence interval based on post-1975 hydrology) is likely near a low-end threshold for the initiation of channel adjustment. The 45,000 cfs flow (approximate 2.5-year recurrence interval based on post-1975 hydrology) was evaluated for continuity with Phase 1 analyses and because it is a frequent flow expected to initiate channel change. The 65,000 cfs flow (approximate 25-year recurrence interval based on post-1975 hydrology) is a likely upper limit of down-valley flood conditions and was modeled to examine relatively infrequent, high flow conditions with significant floodplain flow. This section describes high flow (45,000 cfs and 65,000 cfs) hydrodynamic model simulations conducted assuming steady flow conditions. The downstream stage boundaries for these flows were set at 478 and 480 feet, respectively, based on a best fit regression to measured stage and discharge on the Little Miami River at Milford. The calculated stage increase with flow was decreased slightly when applied to the downstream end of the model to account for increased floodplain storage in the vicinity of the Study Reach. Based on the stage-discharge regression and measured low flow stages in the project reach, the unadjusted elevations for 45,000 and 65,000 cfs flows were 478.09 and 481.47 feet.

Several modifications to the Phase 1 model grid were made in the second phase of the analysis. Modification of the Phase 1 model grid was based on review of the predicted water depths at the channel banks. The lateral coverage of the floodplain was adjusted in an iterative fashion such that the predicted flow depth approached zero at the model boundaries. Also, a review of stage-discharge relationships at upstream discharge gages led to an increase in the downstream stage boundary condition. In the Phase 1 effort, the boundary conditions were set at bank full elevation, but further review of the bathymetry indicated that the location chosen was a low point on the bank and not representative of bank-full elevations. Therefore, the stage was increased by six feet from 472 feet to 478 feet for the 45,000 cfs flow.

Figure 23 presents a comparison of predicted water levels along the channel thalweg for both the Phase 1 and Phase 2 grids (for 45,000 cfs). The expansion of the grid to cover more of the adjacent floodplain, coupled with the increased downstream stage, yielded a more gently sloping water level. Even with the increased stage at the downstream boundary, predicted water levels in Phase 2 are below those reported in Phase 1. Figure 24 presents flow velocities along the channel thalweg for the same simulations shown in Figure 23. The high flow velocities predicted at the downstream boundary in Phase 1 are muted in Phase 2 because of the increased stage at the boundary. The increased lateral width of the floodplain also decreases the predicted centerline velocity from those presented in Phase 1. Peak channel centerline velocities are approximately 8 feet per second in the calibrated model for the 45,000 cfs flow scenario. Overflow onto the floodplain occurs in the upper portion of the model reach through low points in the natural river levee. The increased coverage of the floodplain in the Phase 2 grid can be seen by comparing Figures 25 and 26. These reflect the width of the river at a flow of 45,000 cfs.

Predicted velocities in the model grid are presented in Figure 27. Flow velocities on the floodplain are generally less than 2 feet per second. At the upstream crossing near the railroad bridge, channel centerline velocities are 8 feet per second. Flow vectors are primarily aligned parallel to the channel banks, where velocities are generally between 4 and 5 feet per second. At the downstream crossing, peak centerline velocities are about 6 feet per second, with lower velocities at the channel banks. Velocities are primarily aligned parallel to the river banks, but some flow does re-enter the channel in this area from the floodplain.

The largest flow modeled in Phase 2 was 65,000 cfs. The downstream stage was set at 480 feet for this simulation. Figures 28 and 29 compare model predicted water surface elevations and velocities along the channel centerline for 45,000 cfs and 65,000 cfs conditions. The boundary elevation was two feet higher for the 65,000 cfs simulation; the difference in water level between this run and the 45,000 cfs run decreases in the upstream direction to 1.5 feet at the railroad bridge. The channel centerline velocities are very similar for these two high flow simulations, particularly in the lower half of the project reach below the Horseshoe Bend. The majority of the increased flow is carried by the floodplain, leaving conditions in the river channel similar

between 45,000 cfs and 65,000 cfs simulations. Therefore, from a geomorphic perspective, the channel forming forces are similar between the 45,000 and 65,000 cfs simulations.

Figures 30 and 31 show the predicted water levels and velocities, respectively, throughout the model grid for the 65,000 cfs simulation. The additional flow inundates more of the natural floodplain area on the south bank. Predicted velocities on the floodplain increase slightly with the increased flow, as does the velocity over the natural banks as water leaves the channel and spills onto the floodplain.

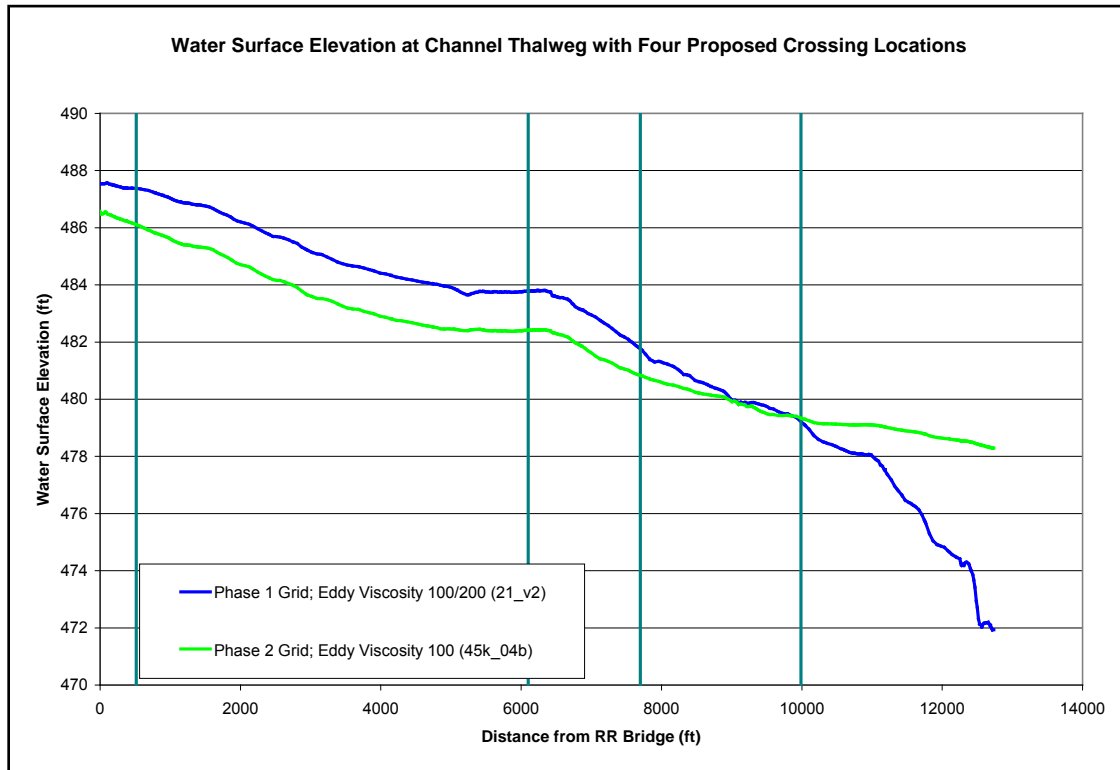


Figure 23. Comparison of Phase 1 and Phase 2 predicted water levels along the channel thalweg

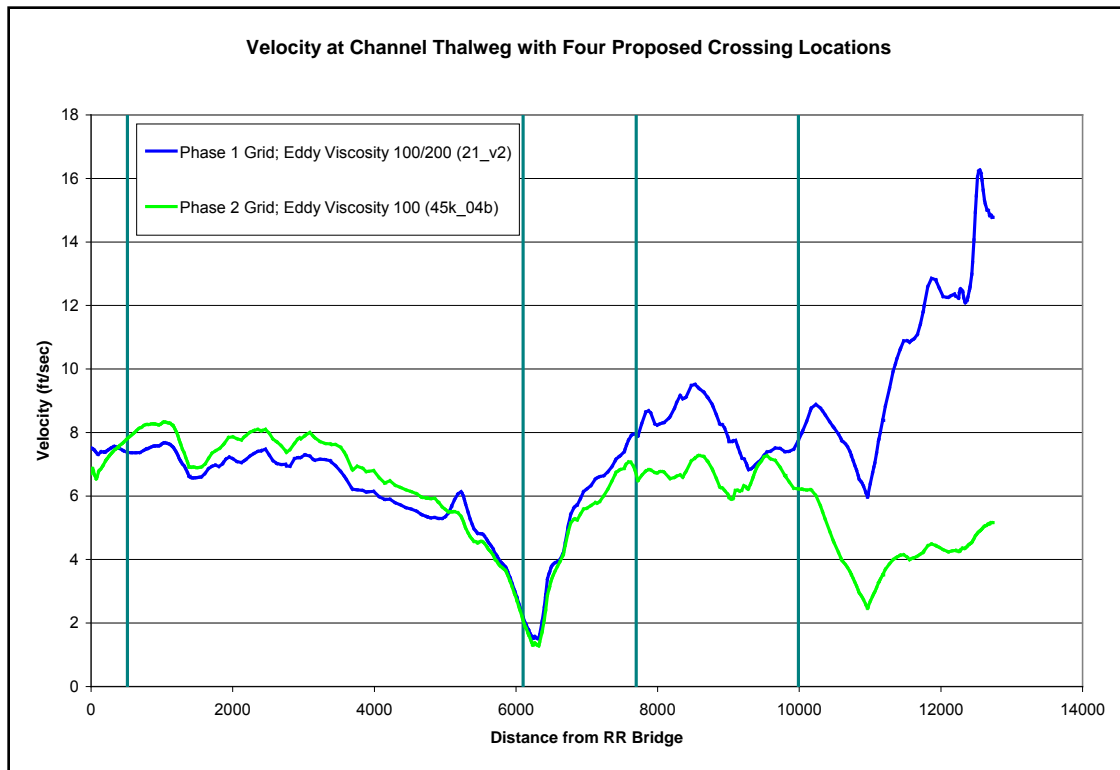


Figure 24. Comparison of Phase 1 and Phase 2 predicted velocity along the channel thalweg

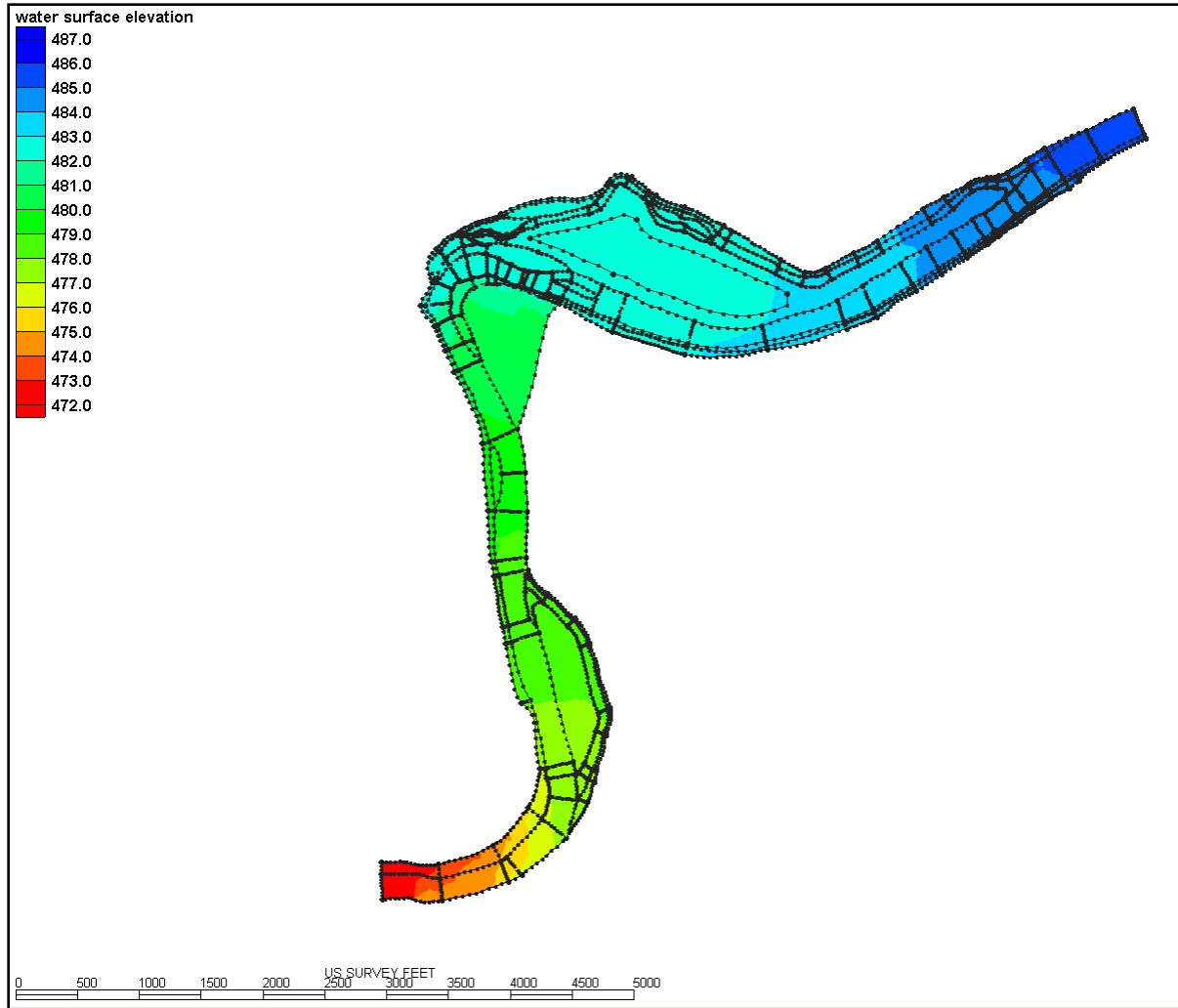


Figure 25. Phase 1 model grid – river elevation and floodplain width at 45,000 cfs

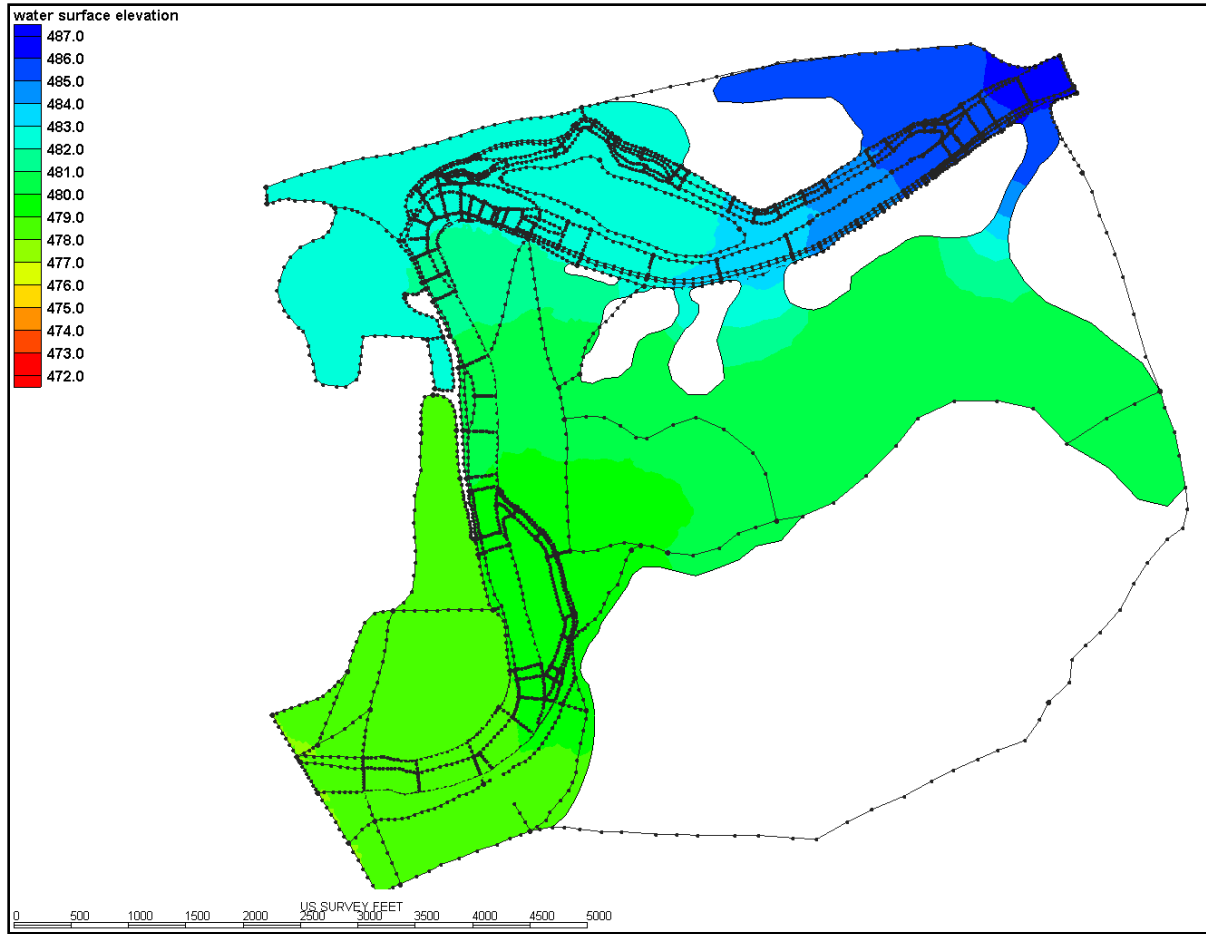


Figure 26: Phase 2 model grid – River elevation and floodplain width at 45,000 cfs

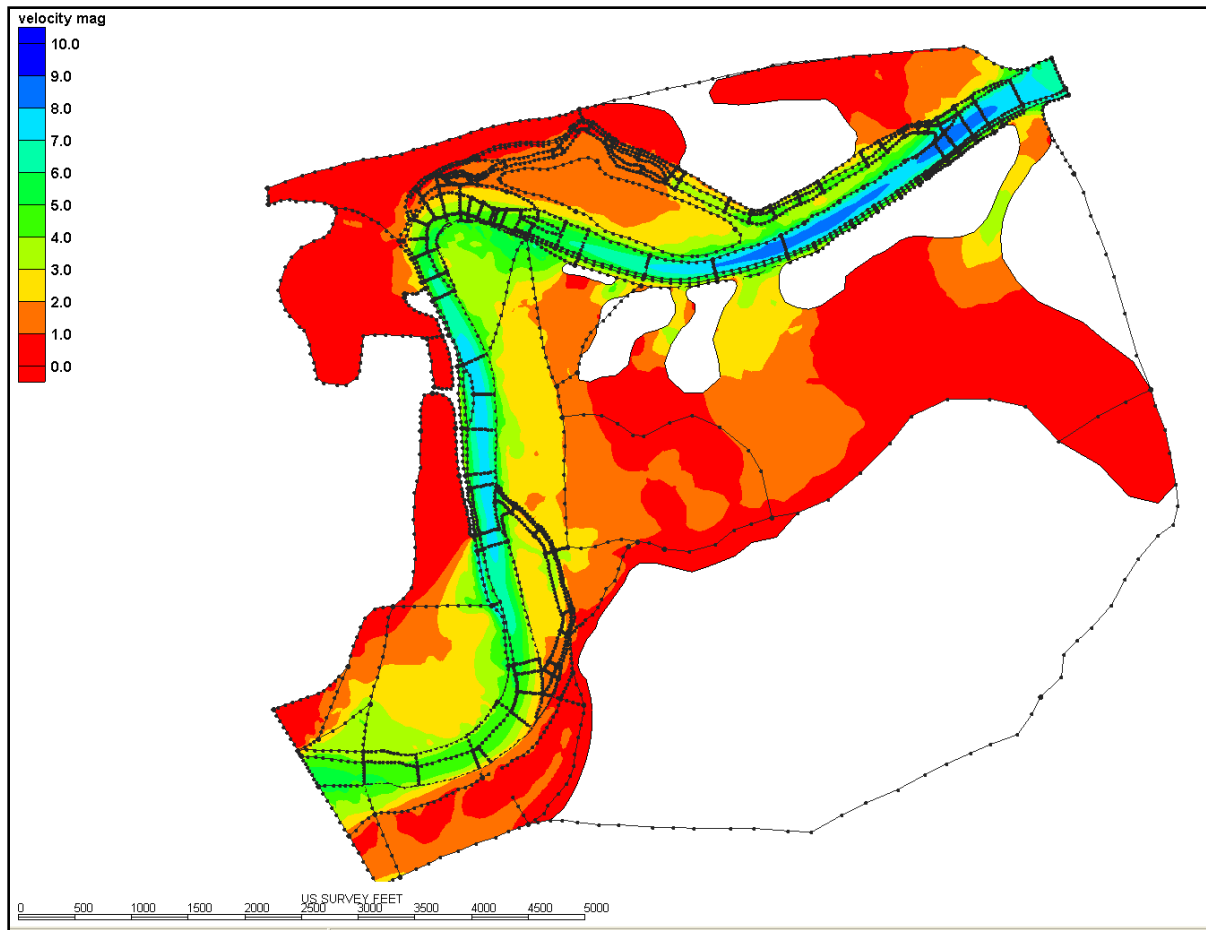


Figure 27. Predicted velocity contours for 45,000 cfs flow (Phase 2 grid)

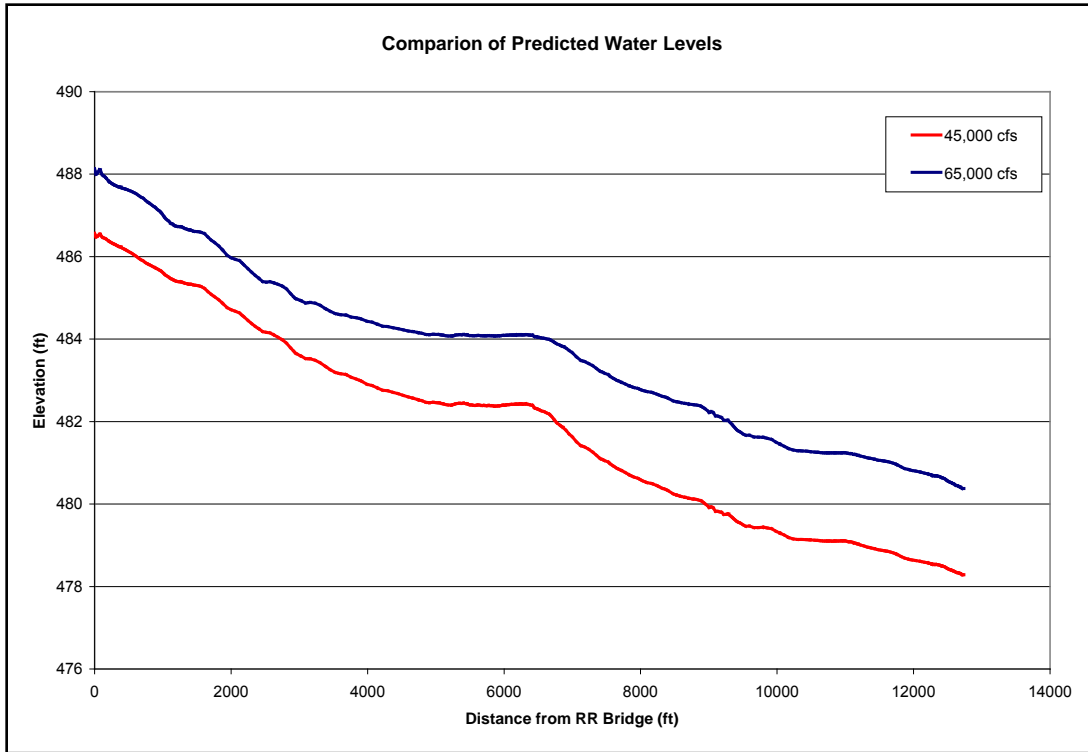


Figure 28: Channel centerline water surface elevations for high flow simulations

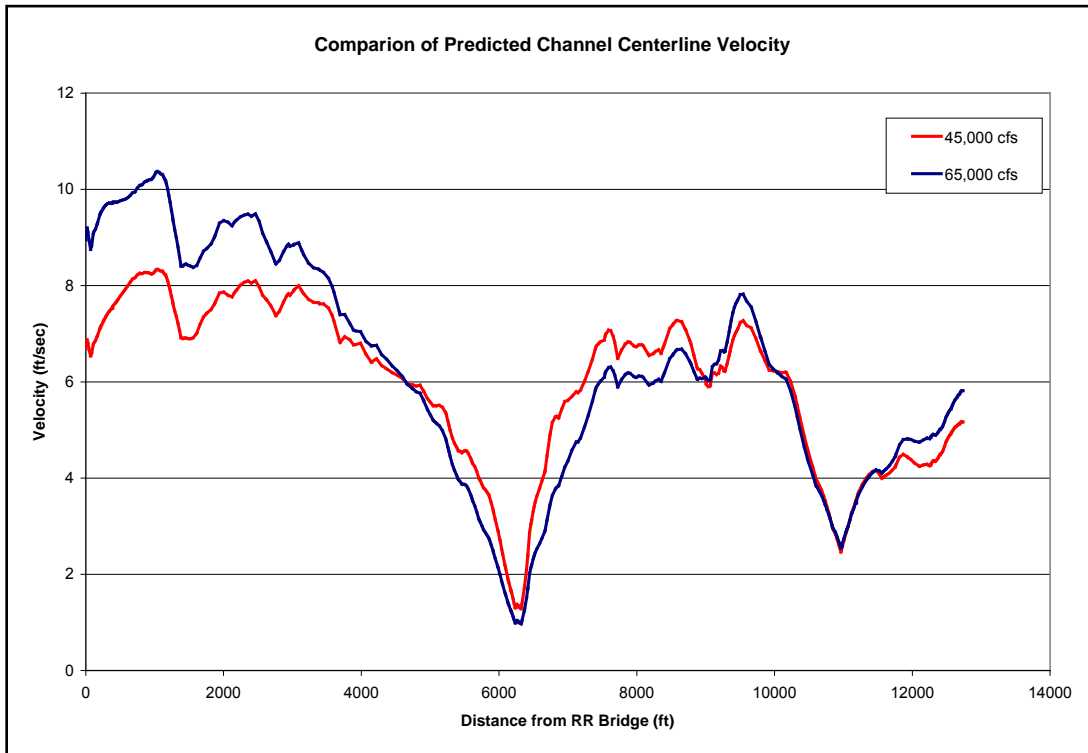


Figure 29. Channel centerline velocity for high flow simulations

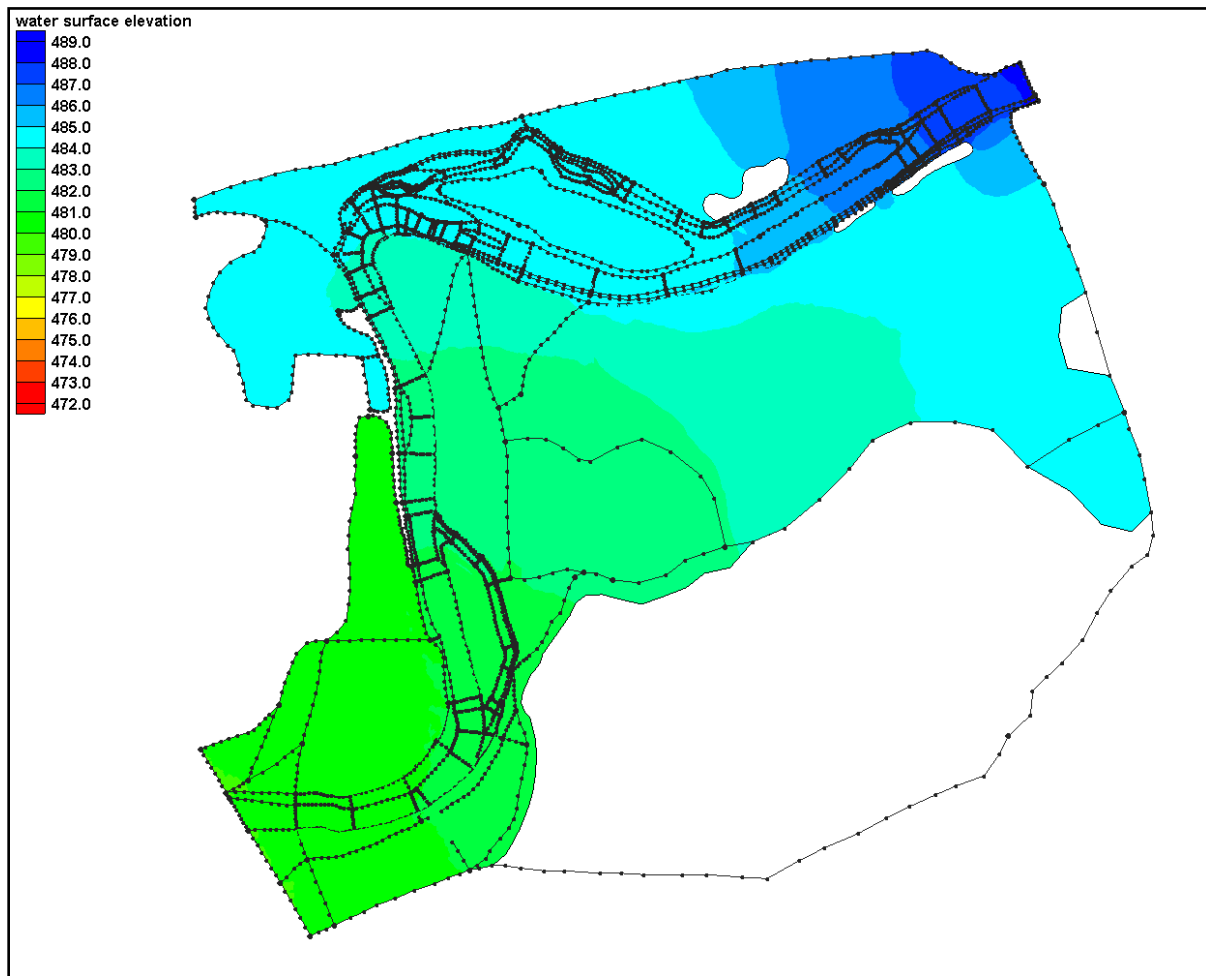


Figure 30. Phase 2 model grid – river elevation and floodplain width at 65,000 cfs

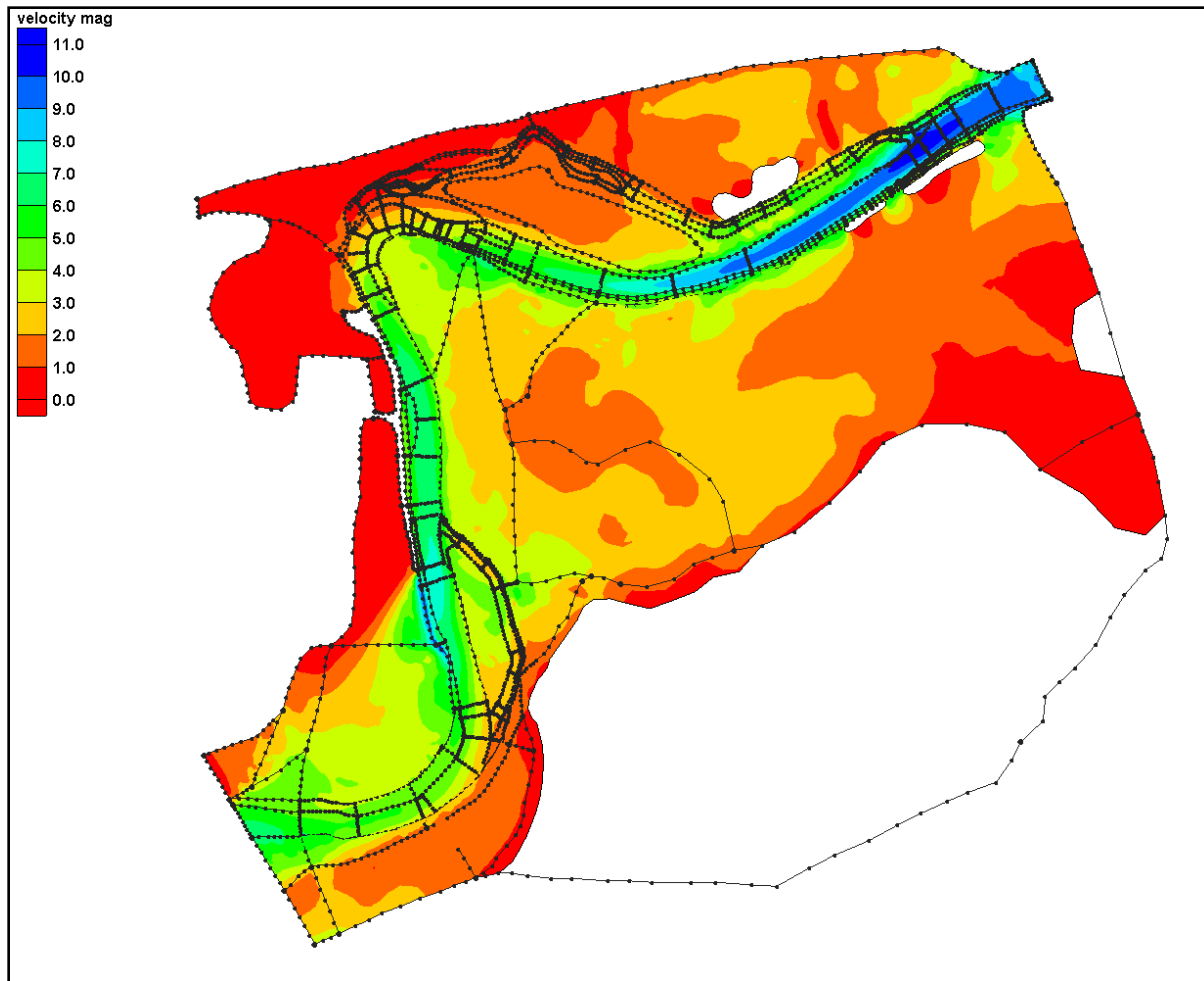


Figure 31: Predicted velocity contours for 65,000 cfs flow (Phase 2 grid)

### 3.5 Sediment Transport Simulations

The SED2D sediment transport model was used to investigate sediment transport in the project reach for 10,000 cfs (approximately 1-year recurrence interval based on post-1975 hydrology), 45,000 cfs (approximately 2.5-year recurrence interval based on post-1975 hydrology), and 65,000 cfs (approximately 25-year recurrence interval based on post-1975 hydrology) to evaluate sediment transport characteristics for a range of flows. The model is capable of predicting the erosion and deposition of both cohesive (silt/clay) and non-cohesive (sand) materials. For this analysis, the focus was on the transport of fine sands as this is representative of the material encountered in the channel banks and on the floodplain in the Study Reach. Channel bank sediment samples were collected at eleven locations along the project reach, and a particle size analysis was conducted to determine the distribution of sediment size in the samples (Stantec 2009b). Table 6 summarizes the results of the analysis, and demonstrates that the bank sediment is primarily fine sand and silt.

**TABLE 6**  
Little Miami River particle size analysis of bank samples – ASTM classification

Classification	Sampling Location Sediment Type Fractions											Ave
	1	2	3	4	5	6	7	8	9	10	11	
Gravel	0.0	0.2	0.0	0.0	0.0	0.0	0.0	0.0	0.8	0.0	39.7	3.7
Coarse Sand	1.2	0.3	0.0	9.2	0.0	0.0	0.0	0.0	0.4	0.0	19.5	2.8
Med Sand	0.5	0.5	0.8	0.2	0.5	0.5	0.5	1.2	5.2	1.5	29.9	3.8
Fine Sand	25.8	29.4	47.3	6.2	10.4	36.0	37.3	87.6	50.8	65.1	2.3	36.2
Silt	51.6	50.3	36.2	55.7	61.1	47.3	45.6	8.0	30.9	26.5	3.7	37.9
Clay	20.9	19.3	15.7	28.7	28.0	16.2	16.6	3.2	11.9	6.9	4.9	15.7

### 3.5.1 Inflow Sediment Concentration

Paired suspended sediment concentration and flow data at Milford were downloaded from the USGS and included a total of 194 measurements collected between January 8, 1975 and September 13, 2000. The peak flow recorded during the collection period for this dataset was 30,194 cfs; however the majority of suspended sediment samples were collected during relatively low flows. Only six samples were taken with flows exceeding 10,000 cfs, and 131 of 194 samples were collected at flows less than 1,000 cfs. This complicates the specification of sediment boundary conditions for the high flow simulations. Figure 32 shows the sediment concentration and discharge dataset. Absent additional data, boundary suspended concentrations were set at 1,000 mg/l for the 45,000 and 65,000 cfs simulations.

### 3.5.2 Model Results

For the high flow simulations (both 45,000 cfs and 65,000 cfs), the model predicts the potential for significant erosion in several regions of the project reach. Based on predicted shear stresses and flow velocities, the greatest potential for erosion occurs in the two long, straight reaches of the channel upstream and downstream of the horseshoe bend (Reaches 4 and 6/7). Contours of potential bed change for the 45,000 cfs simulation are presented in Figure 33. It is extremely important to note that these model results assume that the entire bed is comprised of fine sand. Since the channel bed is actually composed of significantly coarser bed sediment (generally gravel with median particle diameters between 7.6 mm and 18.6 mm), especially at the low flow riffle just upstream of the Horseshoe Bend, model predictions of erosion areas should be interpreted as areas with excess sediment transport capacity that are unlikely to be depositional, rather than areas experiencing ongoing bed scour<sup>1</sup>. This interpretation is supported by the scour chain investigations and bank erosion measurements conducted by Stantec (2009a). Figures 33 and 34 both illustrate sediment transport dynamics in the vicinity of Horseshoe Bend that are conducive to the development of meander cutoffs as described in Section 2.3. During overbank flow conditions, the reach upstream of the Horseshoe Bend appears to be a transport reach while the Horseshoe Bend itself appears to be more depositional. Therefore, as sediment deposits in and adjacent to the Horseshoe Bend it is likely that this could eventually create elevation gradients that would force the main channel to shift during a future high flow.

<sup>1</sup> The sediment transport model used in this study is limited to analyzing the transport of a single sediment size class at a time where successive runs are generally used to investigate separate size classes. The model cannot be used to predict the bed transport in gravel bedded rivers but it can be applied to sand sized and smaller particles. Because the channel banks are primarily comprised of sand, silt and clay sized particles, the model is appropriate for this investigation because a primary goal of this analysis was the channel bank stability.

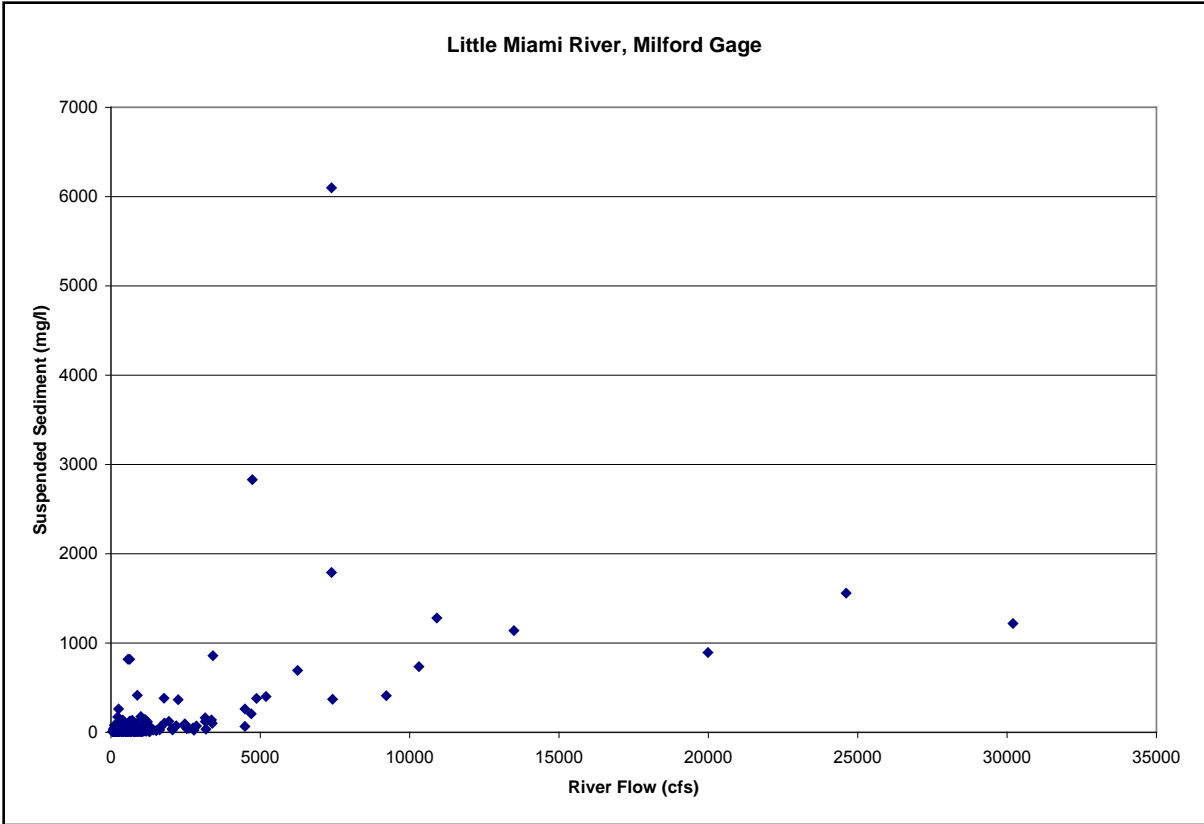


Figure 32. Suspended sediment and flow measurements at Milford Gage

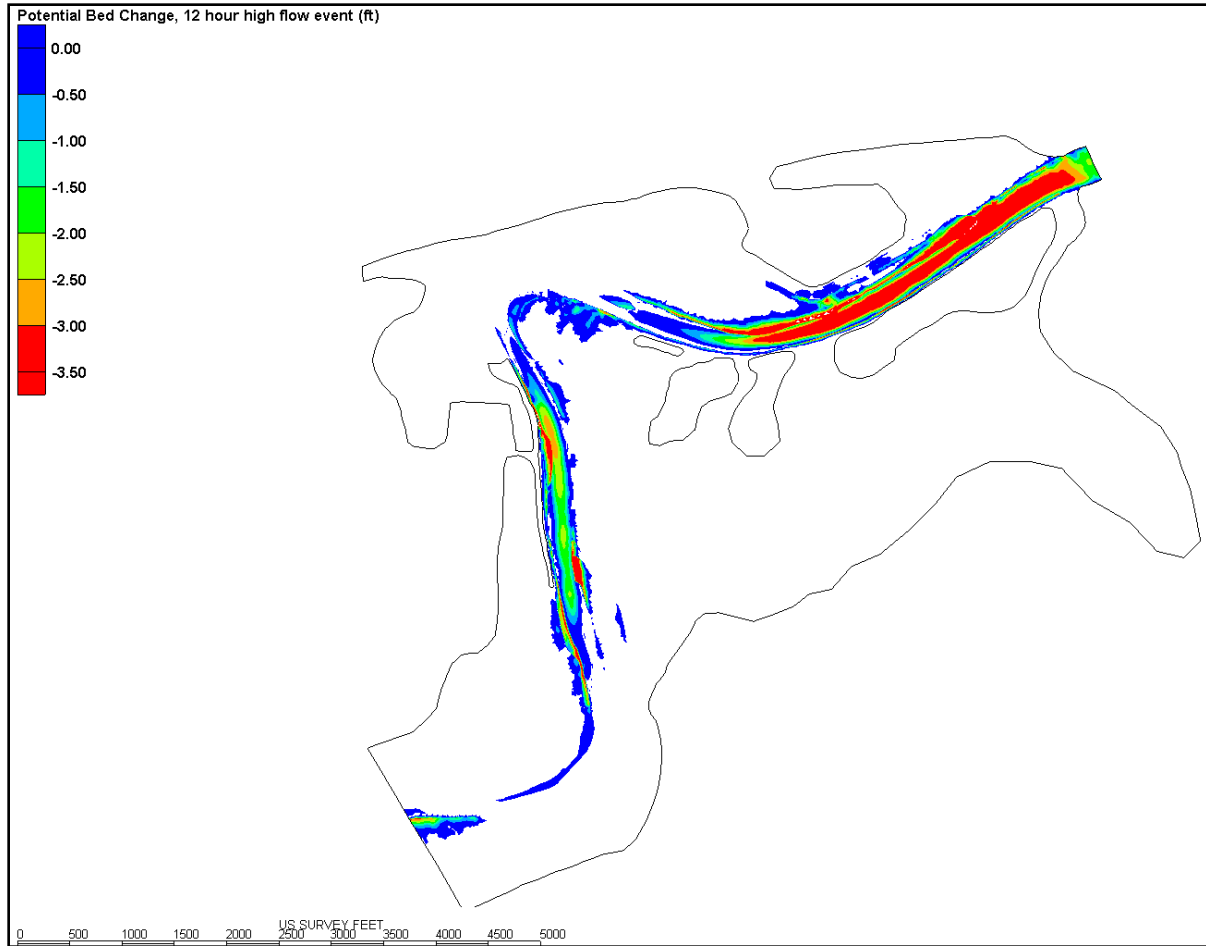


Figure 33. Potential Bed Change Contours for 45,000 cfs (12 hour run with fine sand substrate)

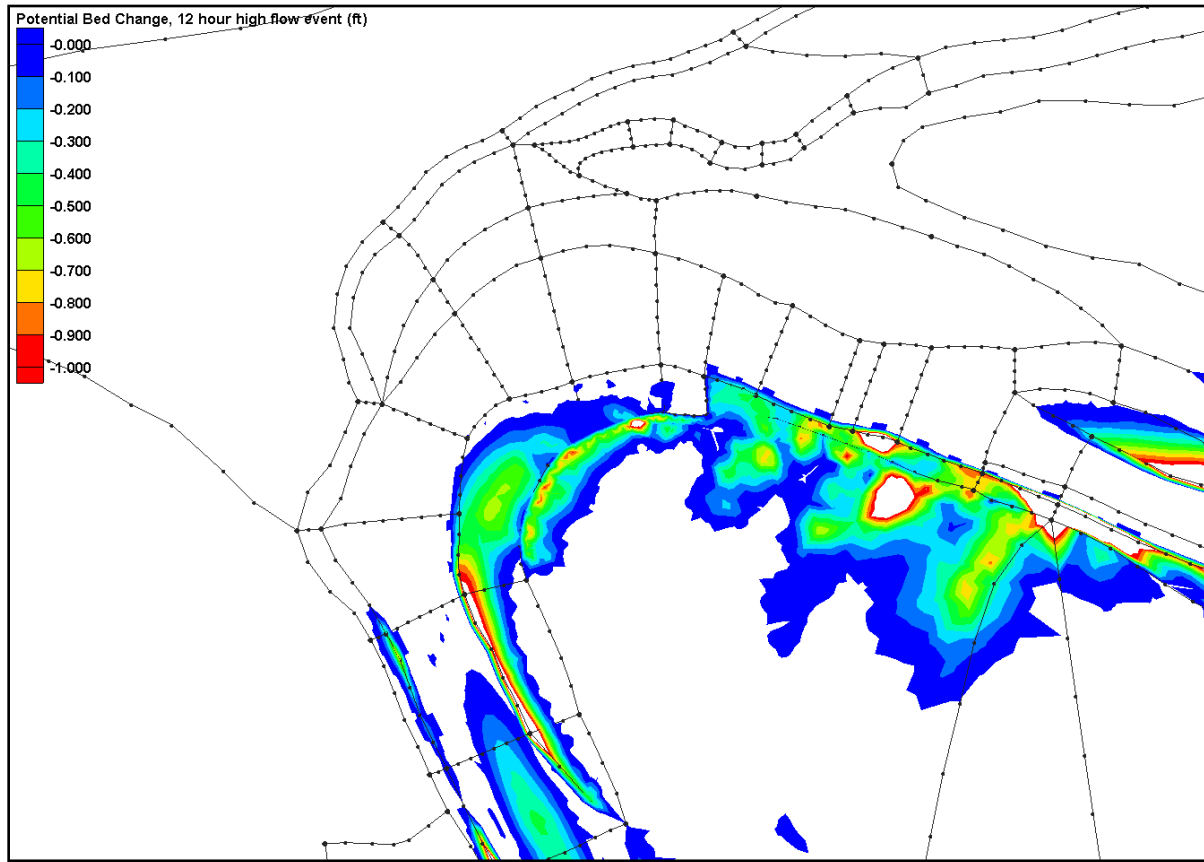


Figure 34. Erosion Patterns in the vicinity of Horseshoe Bend (45,000 cfs)

### 3.6 Geomorphic Interpretation of Hydraulic and Sediment Transport Modeling

Appendix A (Figures A1 – A19) includes plan views of depth, velocity, and shear stress conditions in Geomorphic Reach 4 and Geomorphic Reach 6/7 for 10,000 cfs, 45,000 cfs, and 65,000 cfs flow simulations. Hydraulic model results for 10,000 cfs in Geomorphic Reach 4 (Figures A2-A4) show that the entire flow is contained in the channel, and that depths are uniform in the upstream half of the reach. Flow depth varies more in the downstream half of Geomorphic Reach 4 along the right bank. Velocity and shear stress patterns generally follow depth patterns, with less stable conditions in the downstream half of the reach. However, velocities and shear stresses are not high enough to cause significant channel change at this flow. At 10,000 cfs, the best location for a clear span bridge in Geomorphic Reach 4 is in the upstream half of the reach. In Geomorphic Reaches 6 and 7, hydraulic model results for 10,000 cfs (Figures A5-A7) show a meandering thalweg in Geomorphic Reach 6 and in the upstream half of Geomorphic Reach 7. There is also a high flow channel at the Clear Creek confluence. Velocities are mostly uniform in Geomorphic Reach 6 and in the upstream half of Geomorphic Reach 7. Velocities are higher and more diverse in the downstream half of Geomorphic Reach 7. At 10,000 cfs, conditions for a clear span bridge are best immediately upstream of the Clear Creek confluence with the Little Miami River in Geomorphic Reach 7.

Hydraulic model results for 45,000 cfs in Geomorphic Reach 4 (Figures A8-A10) indicate significant overbank flow across the adjacent floodplain. Flow depth patterns appear similar to the patterns observed in the 10,000 cfs scenario. Velocities and shear stresses are lower in the upstream half of Geomorphic Reach 4 and still below stability thresholds throughout this reach. Geomorphic Reaches 6 and 7 (Figures A11-A13)

also experience significant floodplain flow at 45,000 cfs. Near bank shear stresses are still mostly below stability thresholds and unlikely to cause major bank erosion at this flow. However, complex hydraulic transitions near the Clear Creek confluence at this flow could begin to induce localized bank erosion. Hydraulic conditions in this area change significantly with increasing flow. This would significantly complicate the design of a clear span bridge at this location.

Hydraulic model results for 65,000 cfs in Geomorphic Reach 4 (Figures A14-16) are similar to the results for 45,000 cfs. Flow depths are slightly higher but still cover essentially the same area. Velocities are approximately 2.5 ft/sec greater than at 45,000 cfs but are still relatively low, especially in the upstream half of this reach along the channel margins. Geomorphic Reaches 6 and 7 (Figures A17-A19) also exhibit similar hydraulic characteristics at 65,000 cfs, such as widespread floodplain flow, mostly uniform shear stresses, and complex velocity patterns near the Clear Creek confluence.

## 4 Summary and Recommendations

---

Phase 1 resulted in the characterization of two of the four Geomorphic Reaches in the Study Reach as potentially suitable for a clear span bridge crossing. Phase 2, summarized in this report, updated hydrologic analyses, validated historical channel change analyses, refined geomorphic measurements, expanded evaluation of meander cut-off potential near Horseshoe Bend, and calibrated and refined hydraulic models to provide final guidance on the placement of a clear span bridge over the Wild and Scenic Little Miami River. Based on this more detailed set of analyses, ***Geomorphic Reach 7 no longer appears suitable for a clear span bridge crossing.*** The combination of relatively high average annual channel migration rates near the downstream end of this reach and the influence of a possible meander cutoff at Horseshoe Bend on the upstream end of this reach makes future evolution of channel conditions highly uncertain. Channel conditions appear significantly more stable upstream in Geomorphic Reach 4. Therefore, ***Geomorphic Reach 4 should be given highest priority for a sustainable bridge crossing location.*** For maximum stability and certainty, the clear span bridge should be located in the upstream half of Geomorphic Reach 4. However, it is important to note that roadway approaches to the clear span bridge could impact nearby high flow paths on the floodplain. Therefore, approach sections should be elevated above the active floodplain to the extent possible regardless of the selected clear span bridge location.

## References

---

- CH2M HILL. 2009. Geomorphic and two-dimensional hydraulic modeling evaluation of the Little Miami River in the Eastern Corridor Segment II/III Study Area – Phase One Report. March 2, 2009.
- FHWA. 1986. U. S. Department of Transportation, Federal Highway Administration, 1986. Design of Stable Channels with Flexible Linings. Hydraulic Engineering Circular No. 15. Washington, DC.
- Stantec. 2009a. Phase II feasibility analysis report. Eastern corridor multi-modal projects segment II/III – priority part B work – Little Miami River geomorphic assessment. November 2009.
- Stantec. 2009b. Phase I feasibility analysis report. Eastern corridor multi-modal projects segment II/III – priority part B work – Little Miami River geomorphic assessment. February 17, 2009.
- USACE. 2009. User’s Guide to RMA2 WES version 4.5, US Army Engineer Research and Development Center, Waterways Experiment Station, Coastal and Hydraulics Laboratory. September 2009.

## **Appendix A – Hydraulic Model Plan View Results**

---

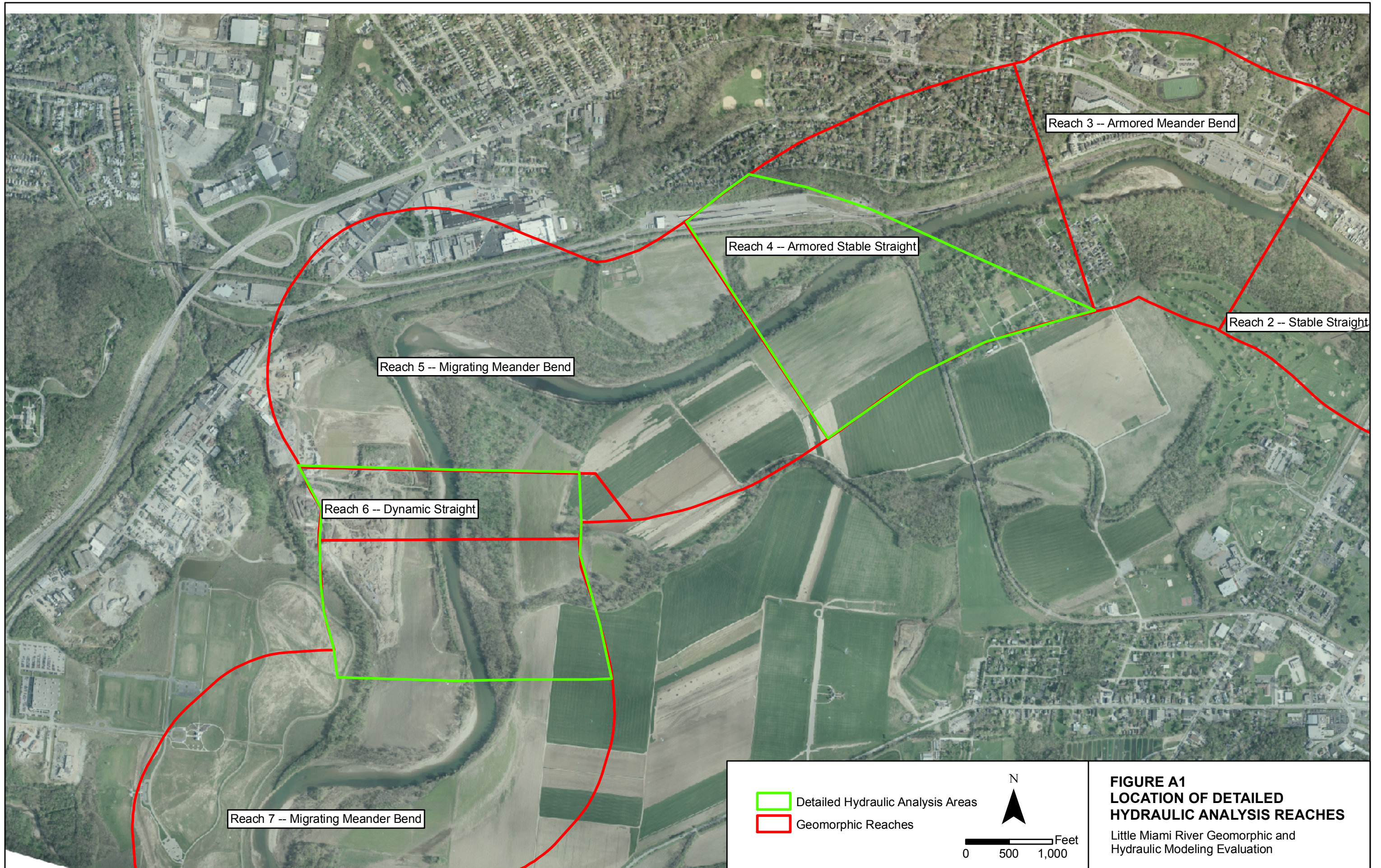
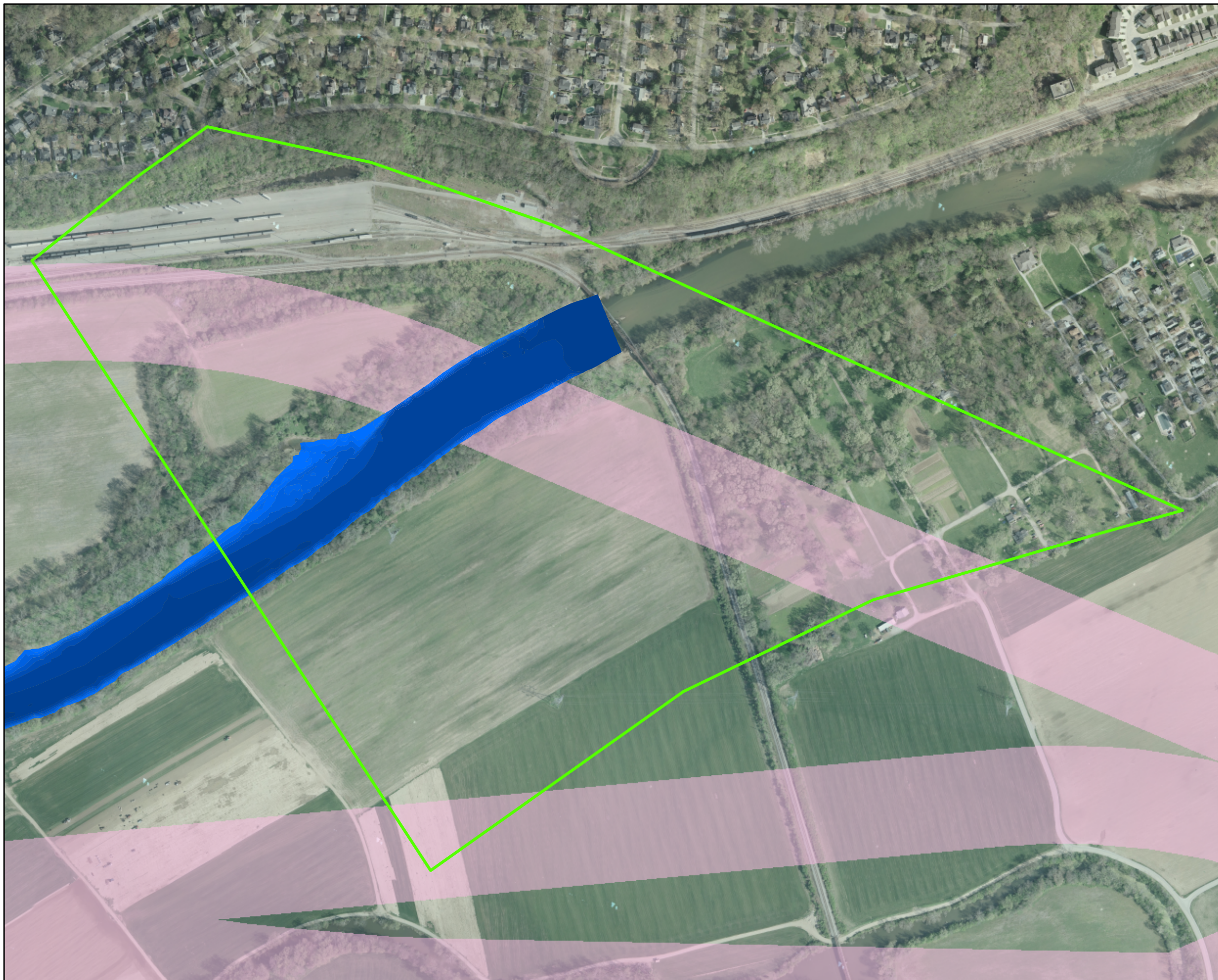


**FIGURE A1**  
**LOCATION OF DETAILED**  
**HYDRAULIC ANALYSIS REACHES**  
 Little Miami River Geomorphic and  
 Hydraulic Modeling Evaluation



**10k Depth (ft)**

- 2
- 3
- 4
- 5
- 6
- 7
- 8
- 9
- 10
- 11
- 12
- 14
- 16
- 18

- Geomorphic Reach 4
- Segment II/III Alternatives



**FIGURE A2**  
**DISTRIBUTION OF DEPTH AT**  
**10,000 CFS GEOMORPHIC REACH 4**  
 Little Miami River Geomorphic and  
 Hydraulic Modeling Evaluation, Phase II

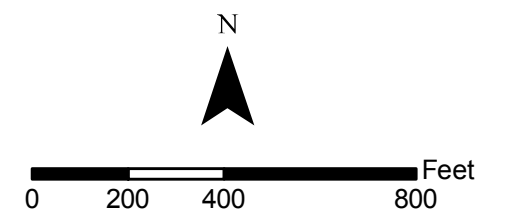
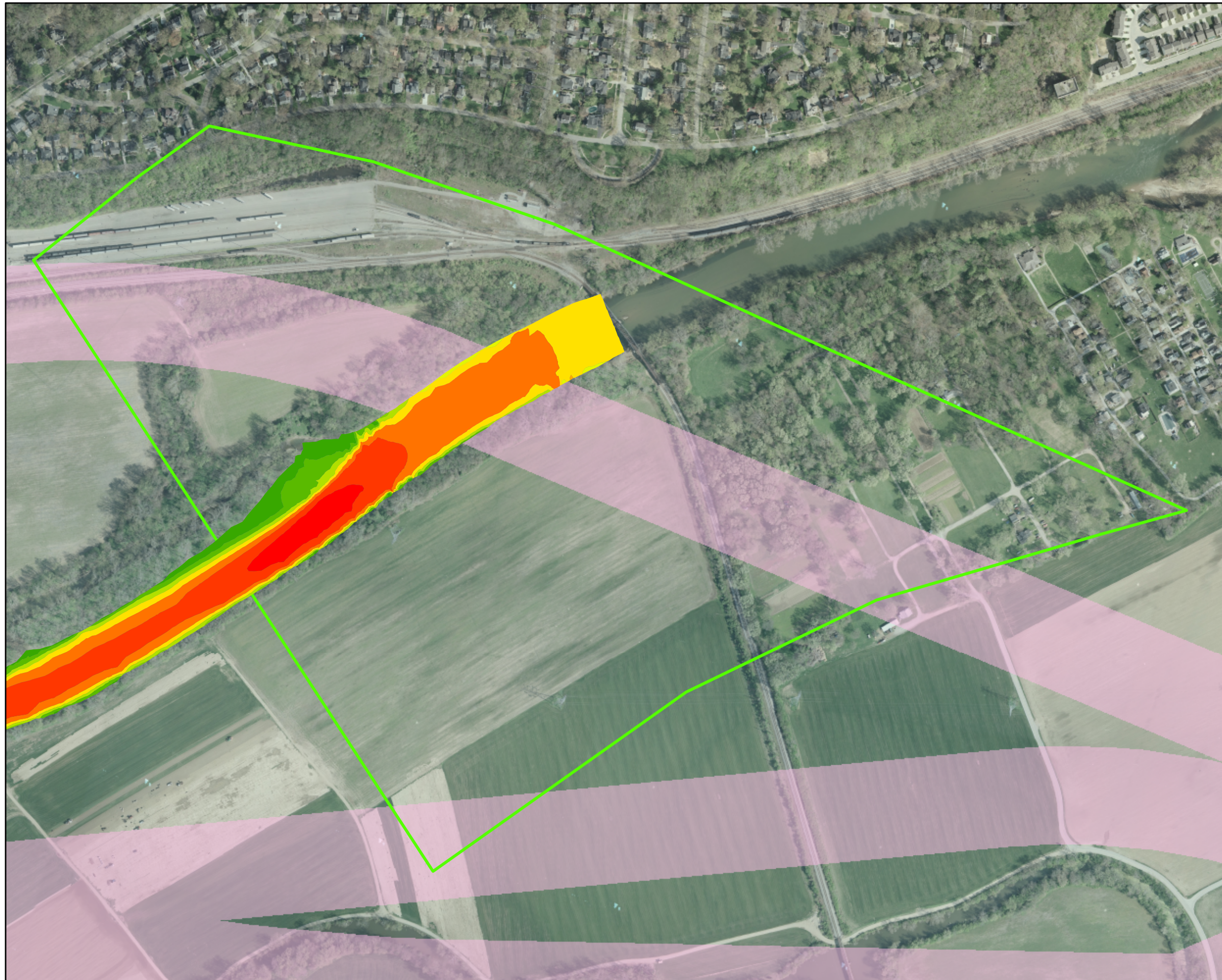
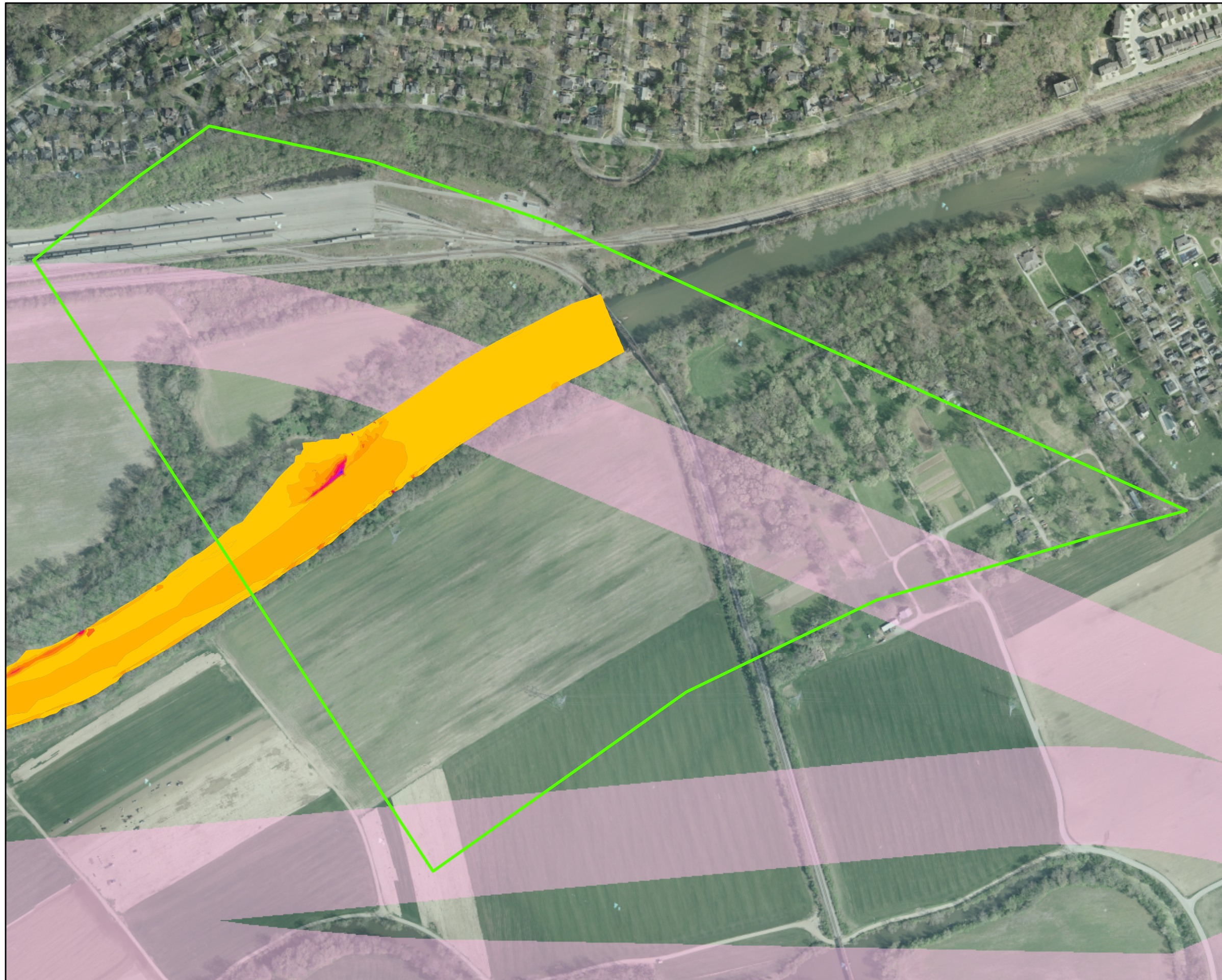


**FIGURE A3**  
**DISTRIBUTION OF VELOCITY AT**  
**10,000 CFS GEOMORPHIC REACH 4**  
 Little Miami River Geomorphic and  
 Hydraulic Modeling Evaluation, Phase II



**10k Bed Shear (N/m<sup>2</sup>)**

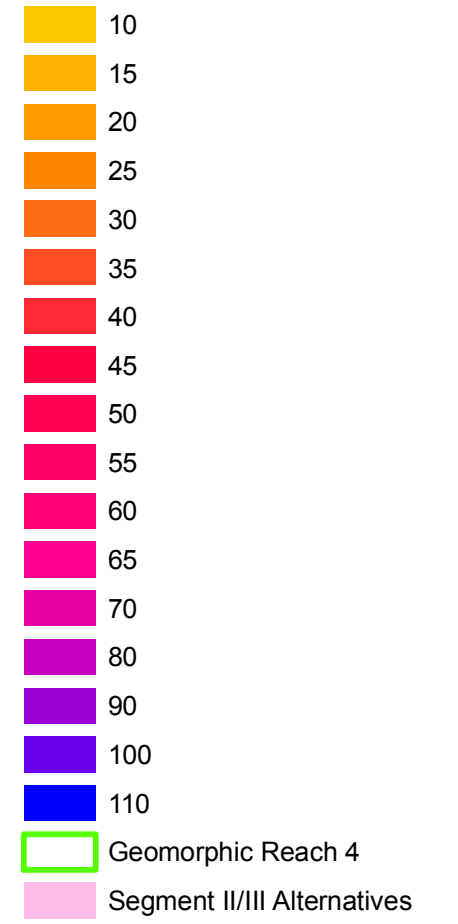
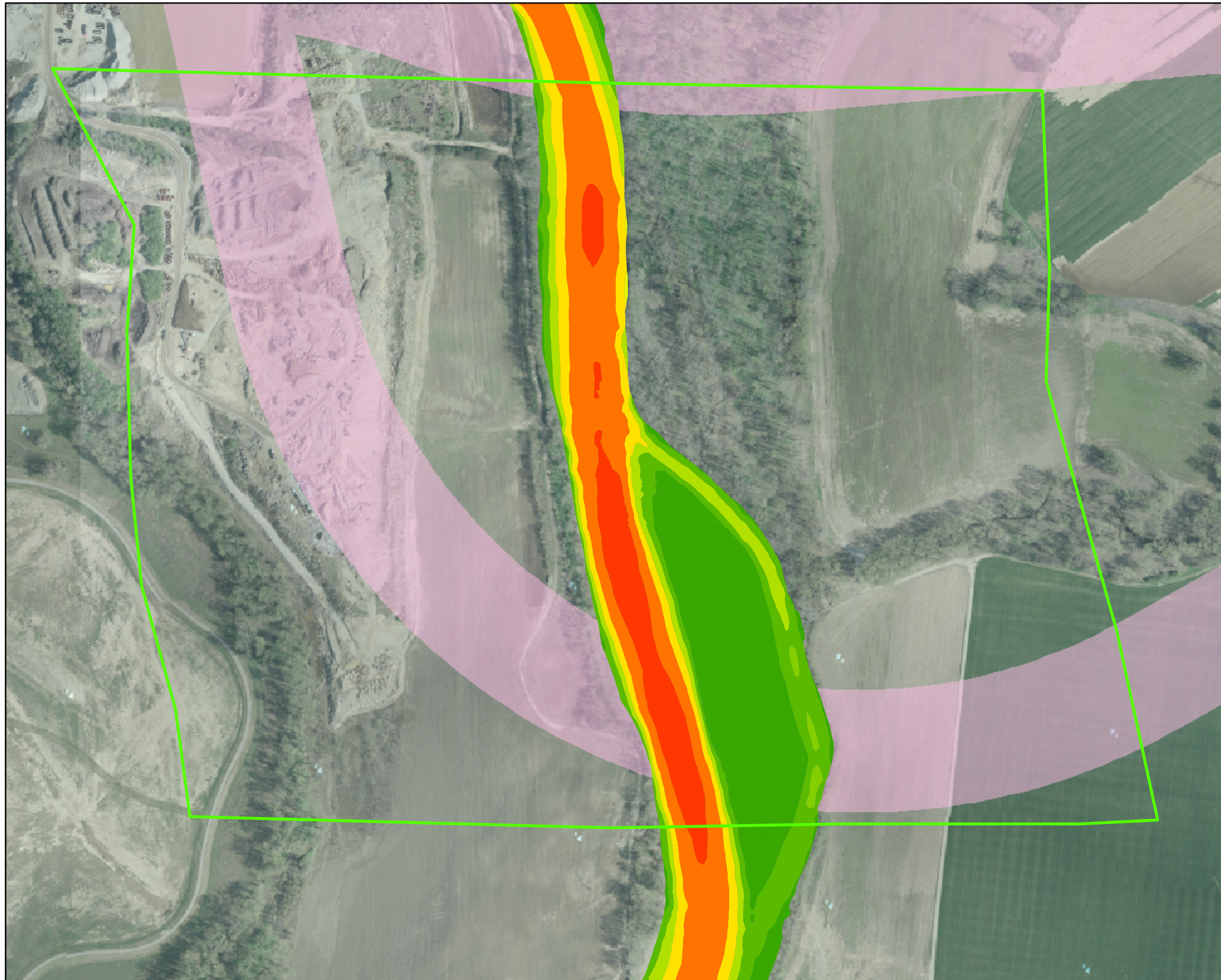


**FIGURE A4**  
**DISTRIBUTION OF BED SHEAR**  
**STRESS AT 10,000 CFS**  
**GEOMORPHIC REACH 4**  
 Little Miami River Geomorphic and  
 Hydraulic Modeling Evaluation, Phase II



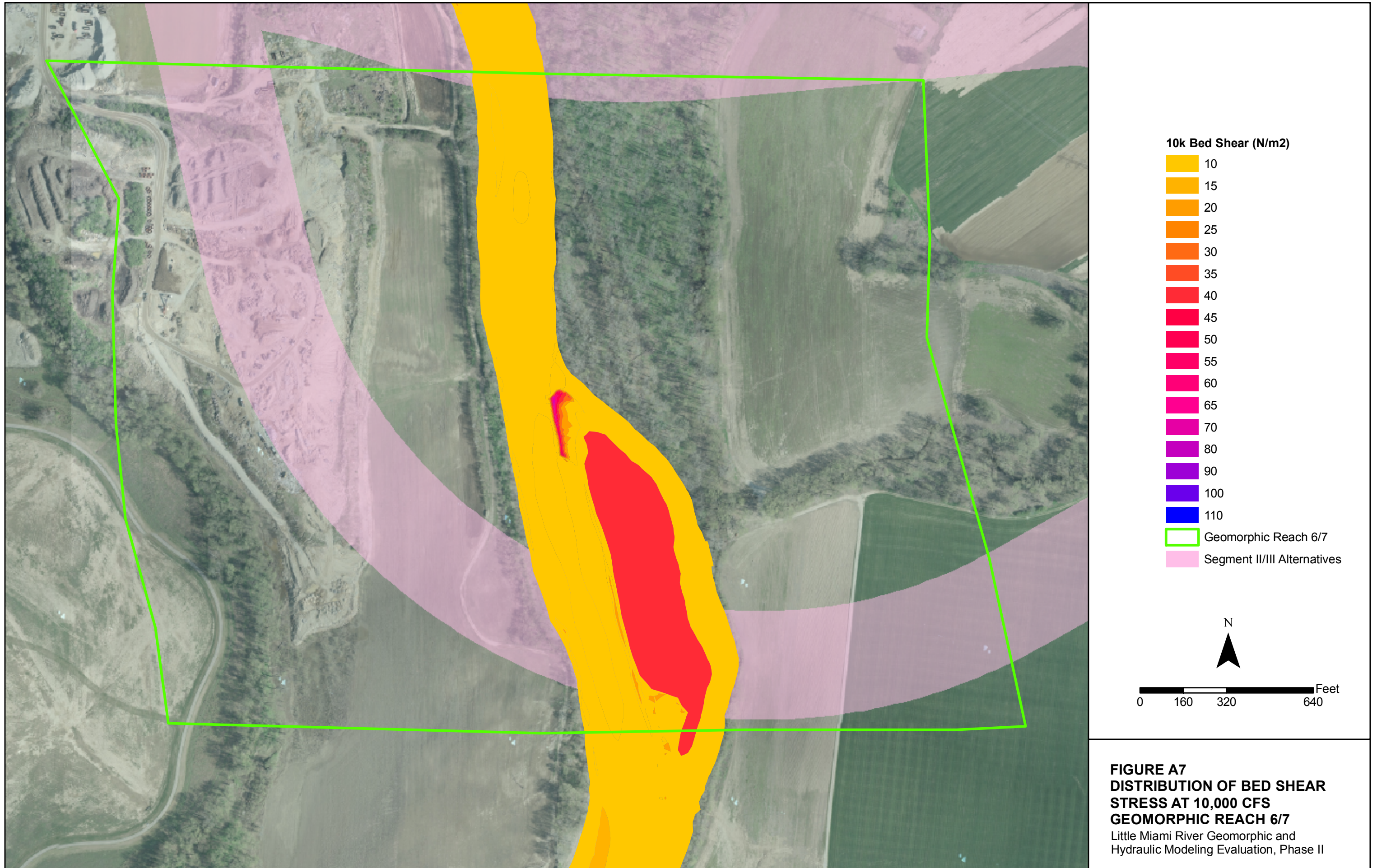


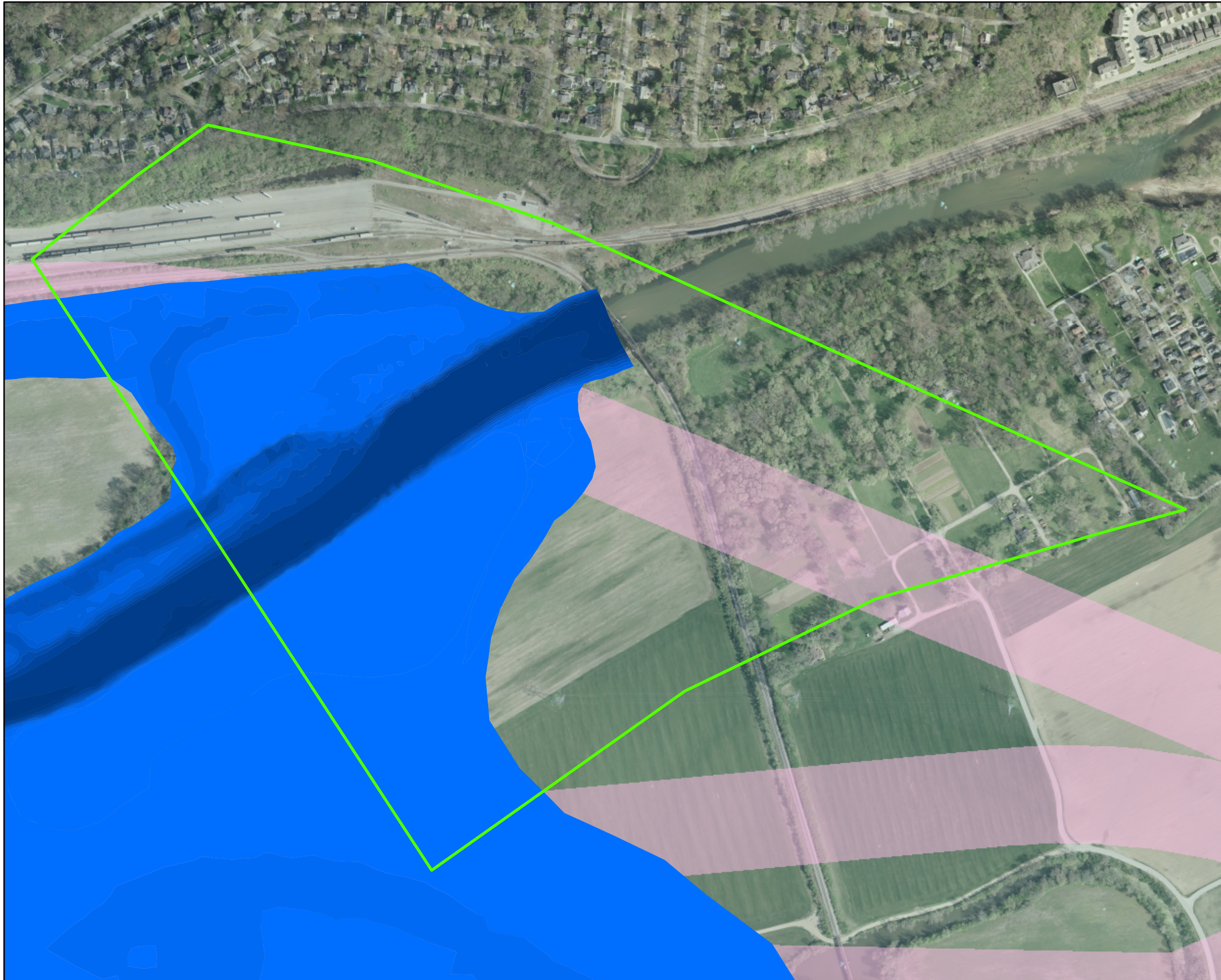
**10k Velocity (ft/s)**

- 1
- 1.5
- 2
- 2.5
- 3
- 3.5
- 4
- 4.5
- 5
- 6
- Geomorphic Reach 6/7
- Segment II/III Alternatives



**FIGURE A6**  
**DISTRIBUTION OF VELOCITY**  
**AT 10,000 CFS**  
**GEOMORPHIC REACH 6/7**  
 Little Miami River Geomorphic and  
 Hydraulic Modeling Evaluation, Phase II





**45k Depth (ft)**

- 1
- 2.5
- 4
- 5.5
- 7
- 8.5
- 10
- 11.5
- 13
- 14.5
- 16
- 17.5
- 19
- 20.5
- 22
- 25
- 28

- Geomorphic Reach 4
- Segment II/III Alternatives



**FIGURE A8**  
**DISTRIBUTION OF DEPTH**  
**AT 45,000 CFS**  
**GEOMORPHIC REACH 4**  
 Little Miami River Geomorphic and Hydraulic Modeling Evaluation, Phase II

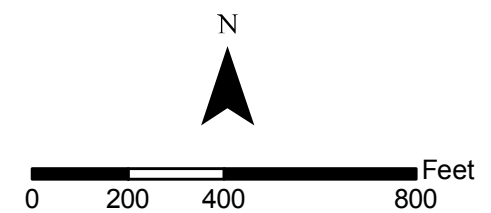
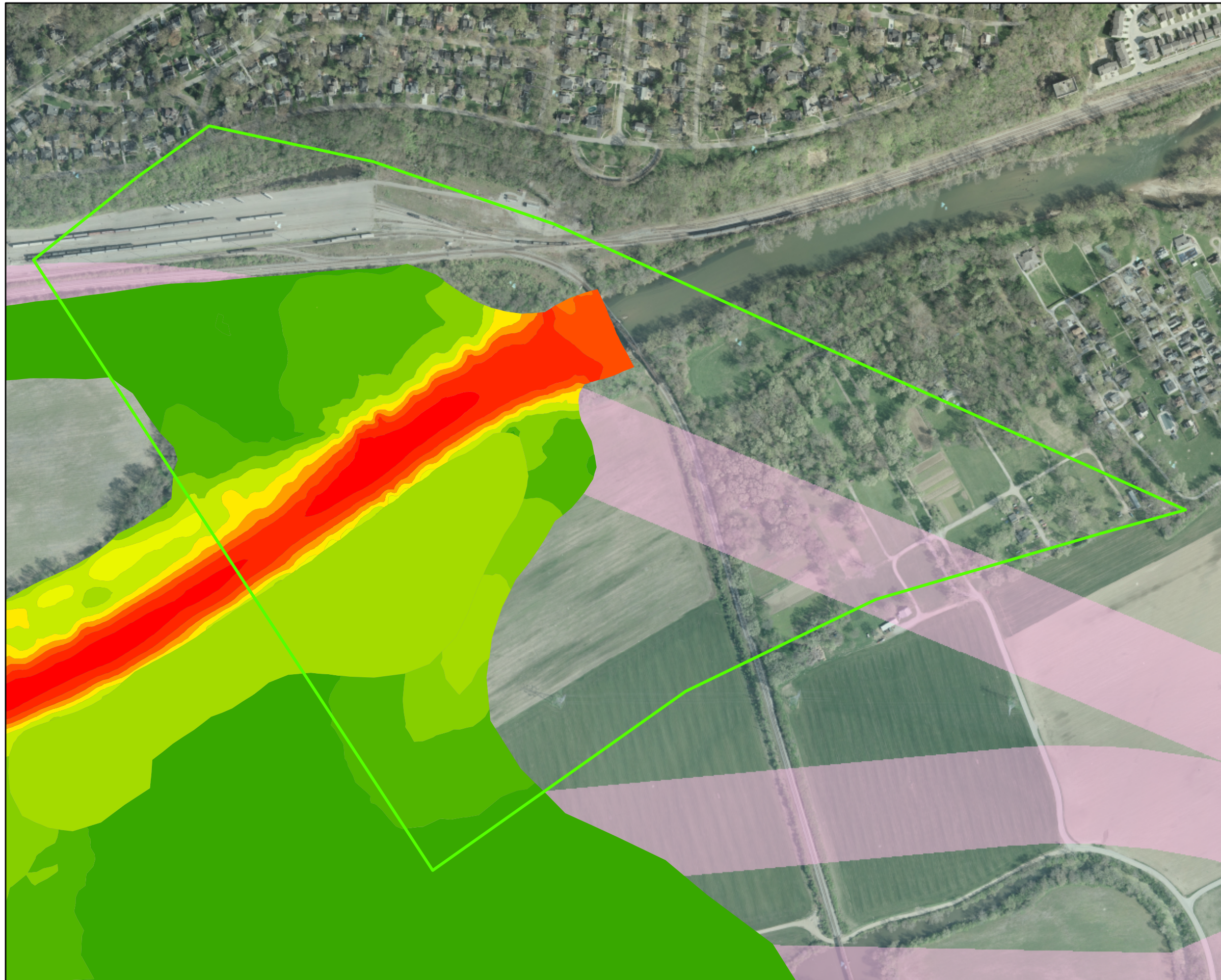
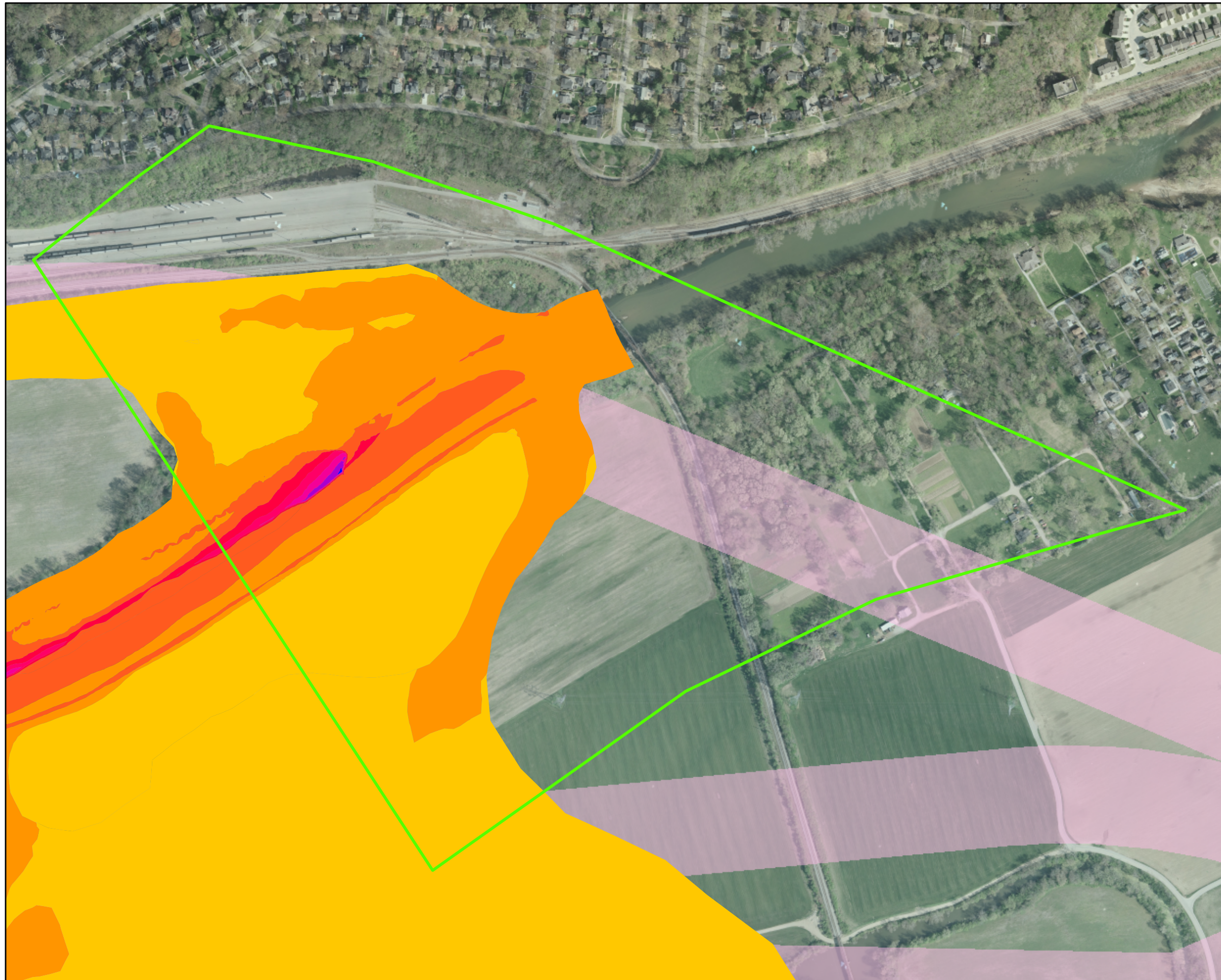


**FIGURE A9**  
**DISTRIBUTION OF VELOCITY**  
**AT 45,000 CFS**  
**GEOMORPHIC REACH 4**  
 Little Miami River Geomorphic and Hydraulic Modeling Evaluation, Phase II



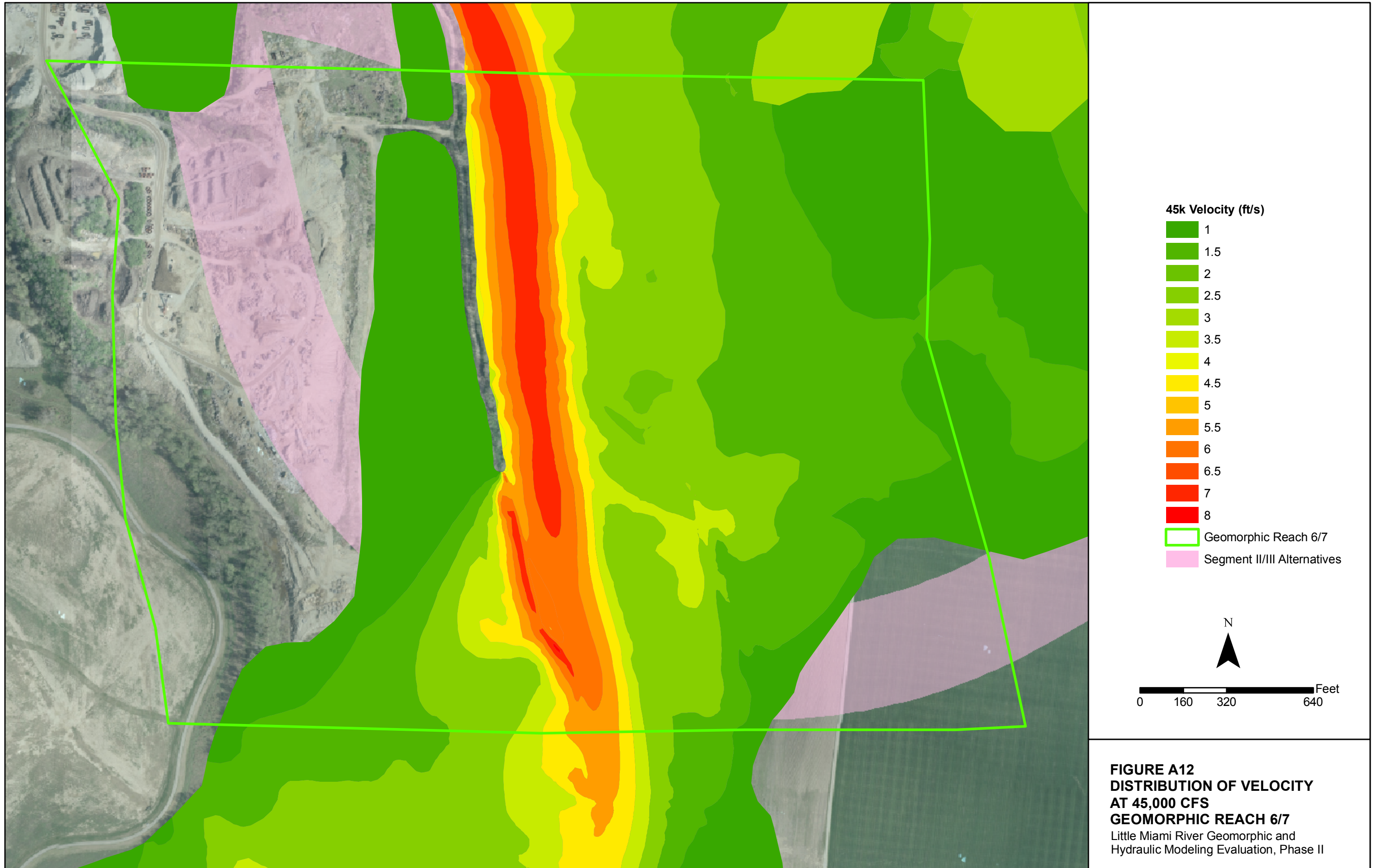
**45k Bed Shear (N/m<sup>2</sup>)**

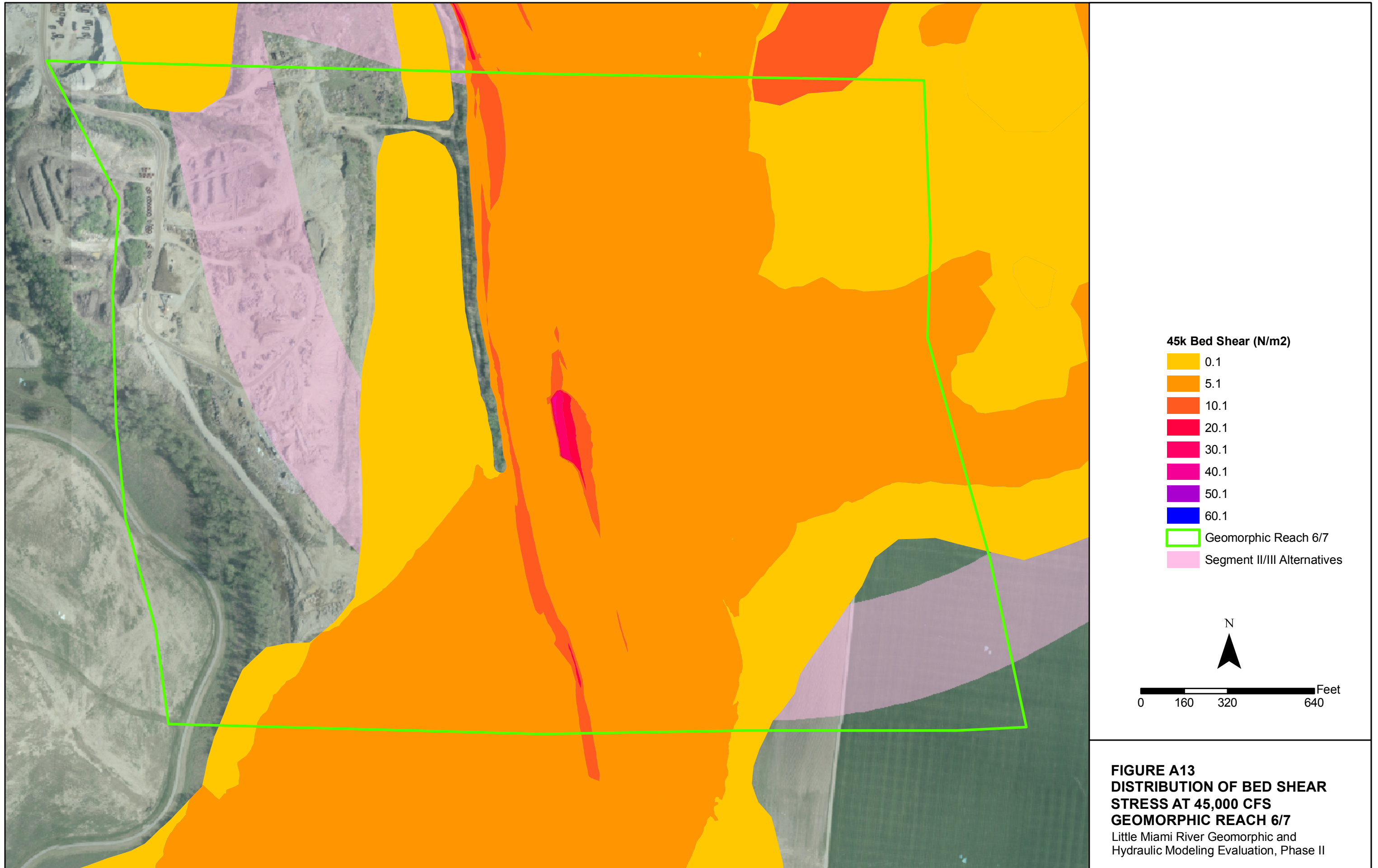
- 0.1
- 5.1
- 10.1
- 20.1
- 30.1
- 40.1
- 50.1
- 60.1
- Geomorphic Reach 4
- Segment II/III Alternatives

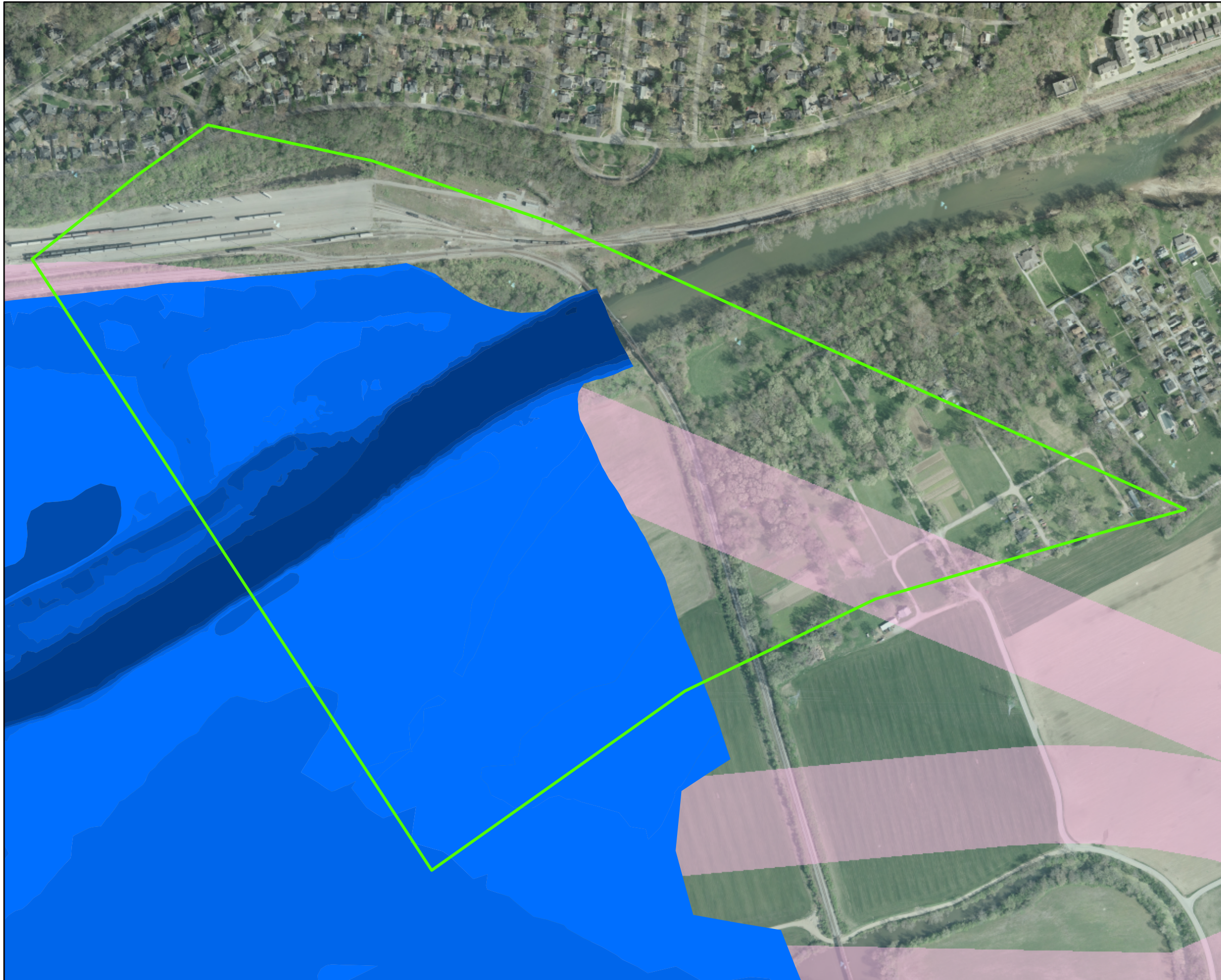


**FIGURE A10**  
**DISTRIBUTION OF BED SHEAR**  
**STRESS AT 45,000 CFS**  
**GEOMORPHIC REACH 4**  
 Little Miami River Geomorphic and  
 Hydraulic Modeling Evaluation, Phase II









**65k Depth (ft)**

- 2
- 5
- 8
- 11
- 14
- 17
- 20
- 26

- Upstream Reach
- Segment II/III Alternatives



**FIGURE A14**  
**DISTRIBUTION OF DEPTH**  
**AT 65,000 CFS**  
**GEOMORPHIC REACH 4**  
 Little Miami River Geomorphic and  
 Hydraulic Modeling Evaluation, Phase II

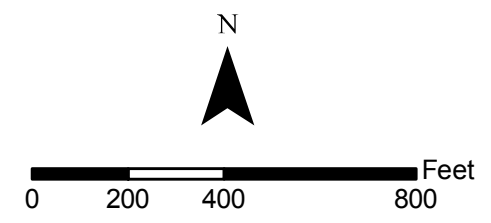
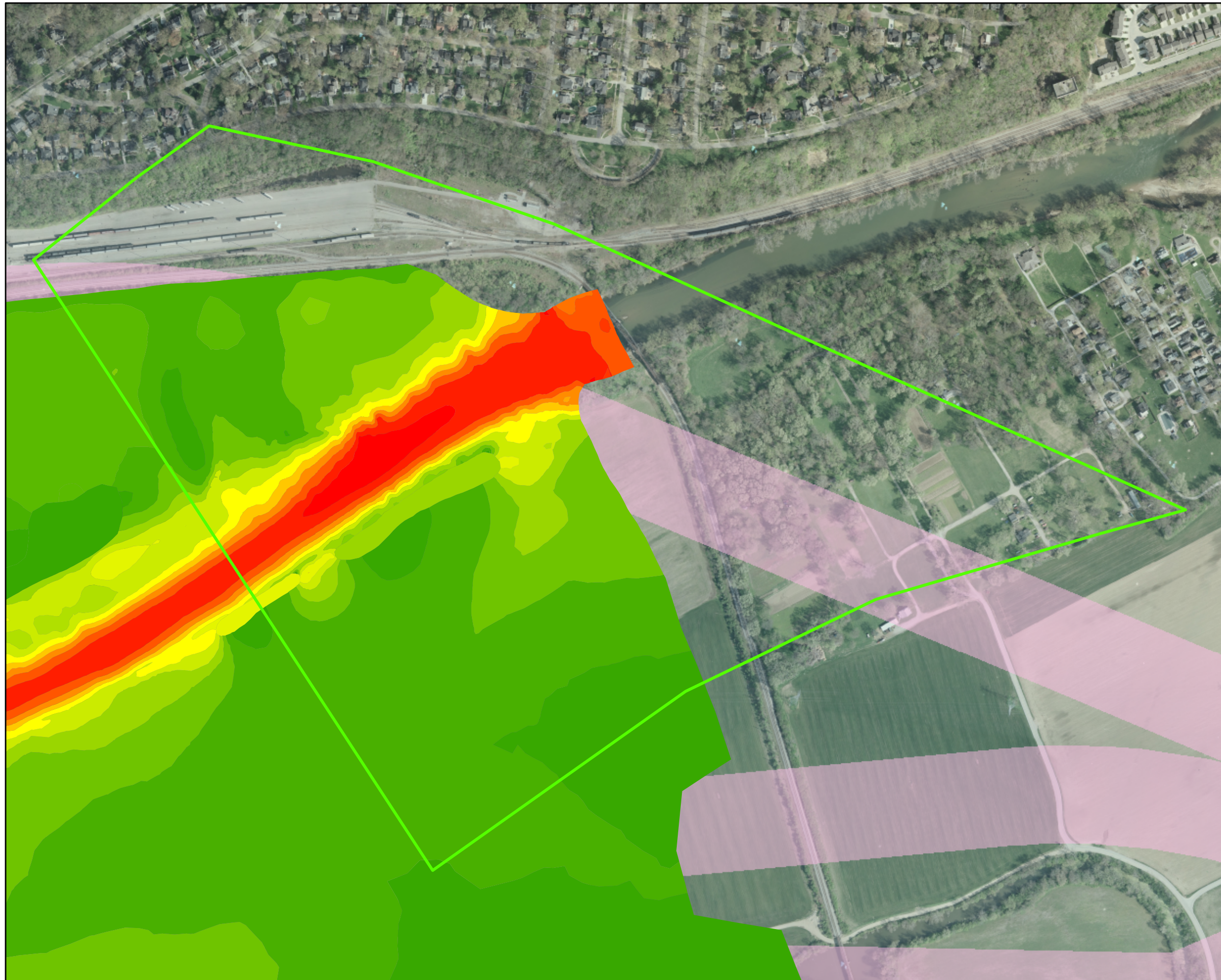


**FIGURE A15**  
**DISTRIBUTION OF VELOCITY**  
**AT 65,000 CFS**  
**GEOMORPHIC RAECH 4**  
 Little Miami River Geomorphic and  
 Hydraulic Modeling Evaluation, Phase II

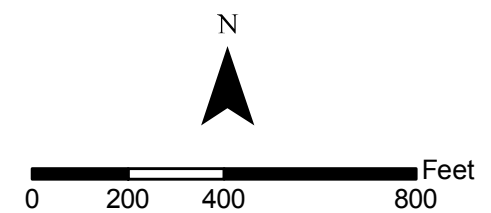
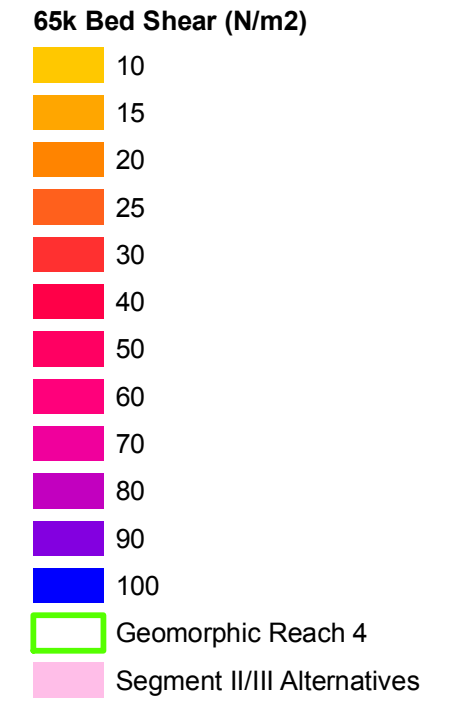
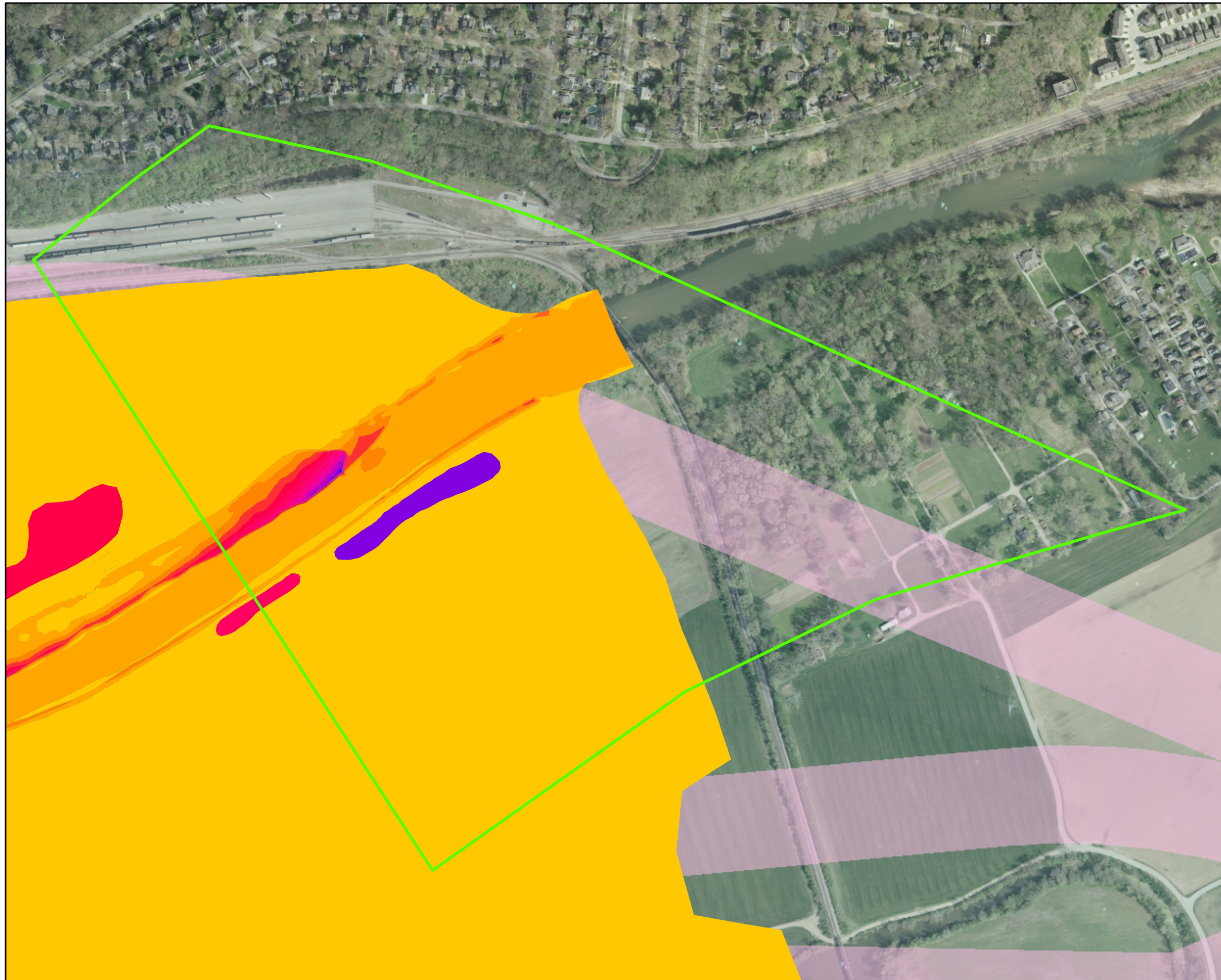


**FIGURE A16**  
**DISTRIBUTION OF BED SHEAR**  
**STRESS AT 65,000 CFS**  
**GEOMORPHIC REACH 4**  
 Little Miami River Geomorphic and  
 Hydraulic Modeling Evaluation, Phase II

